EXPLORING THE CONTRIBUTION OF THE MAGNOCELLULAR PATHWAY IN FILLING-IN OF ARTIFICIAL SCOTOMA

by

SHRUTI NARANG

(Under the Direction of James M. Brown)

ABSTRACT

Perceptual illusions and disorders often provide insights into normal visual mechanisms. Artificial scotoma is a type of illusion where our visual system loses perception of a peripheral target on a dynamic noise background over several seconds. Several studies have shown that specific sensory manipulations like the size of target and background temporal variations affects the time taken for a target to fade. There is no unifying theory to account for the sensory factors that play a major role in determining the length of time taken to fade. The experiments described here explored the relation between sensory factors preferentially processed by the magnocellular pathway and the time taken to induce a scotoma. In addition to measuring time taken to fade, the duration of time a target stayed invisible was also measured. The two measures were recorded for conditions that either stimulate the magnocellular pathway or reduced its response relative to engaging the parvocellular pathway. The results indicate that altering the background characteristics by using different flicker rates, diffuse red light, and a background pulsed pedestal affected time to fade and the probability of fading. The spatial frequency within the target region affected the duration of fading. Time taken to fade seems to be modulated by background characteristics while the time taken to reappear seems to be more modulated by target region

characteristics indicating the role of competition between figure and ground. The results provide strong support for the role of visual pathways and figure-ground segregation mechanisms in the perceptual filling-in of a scotoma.

INDEX WORDS: Magnocellular and Parvocellular Visual Pathways, Artificial Scotoma, Perceptual Filling-in, Figure-Ground Segregation, Texture, Contrast

EXPLORING THE CONTRIBUTION OF THE MAGNOCELLULAR PATHWAY IN FILLING-IN OF ARTIFICIAL SCOTOMA

by

SHRUTI NARANG

B.A., University of Allahabad, India, 2005

M.A., CBCS, University of Allahabad, India, 2007

A Dissertation Submitted to the Graduate Faculty of The University of Georgia in Partial Fulfillment of the Requirements for the Degree

DOCTOR OF PHILOSOPHY

ATHENS, GEORGIA

2014

EXPLORING THE CONTRIBUTION OF THE MAGNOCELLULAR PATHWAY IN FILLING-IN OF ARTIFICIAL SCOTOMA

by

SHRUTI NARANG

Major Professor: James M. Brown

Committee: Billy R. Hammond
Jennifer E. McDowell

Electronic Version Approved:

Julie Coffield
Interim Dean of the Graduate School
The University of Georgia
August 2014

ACKNOWLEDGEMENTS

I would like to take this opportunity to express my profound gratitude and deep regards to my advisor, Dr. James M. Brown, for his support and mentorship throughout this process. I would like to thank him especially for the numerous critiques and comments suggested to me during the writing process. I would also like extend my appreciation to the other members of my committee, Dr. B. Randy Hammond and Dr. Jennifer E. McDowell for their advisement on this project. The completion of my thesis would not have been possible without the support and guidance of my major professor and my committee. Lastly, I thank my family, friends, and colleagues for their love and encouragement. Thank you.

TABLE OF CONTENTS

LIST OF FIGURES

Page

CHAPTER 1

INTRODUCTION

Human visual experience often suffers from inaccuracies due to limitations in visual processing. Nevertheless, we have evolved to interpret the available visual resources to maximize our phenomenological experience. For example, we encounter occluded objects during our daily activities and to resolve for the physically absent information, our visual system has developed interpolation techniques to fill such gaps in visual space. Scotomas and blind spots are other forms of such visual gaps. On occasion, pathological conditions such as a scar on the retina can result in a scotoma. Such scotomas are referred to as retinal or pathological scotomas. Scotomas can also be *induced* using specific types of stimuli and hence are termed as artificial, perceptual, or induced scotomas. Studies on the artificial scotoma, the blind spot, and the pathological scotoma phenomenon have found some similarities in the underlying filling-in process involved.

The literature on the artificial scotoma has addressed what stimulus characteristics induce a scotoma, but there is no unanimous agreement on why it occurs. The major explanations proposed include, (A) boundary adaptation (Ramachandran, Gregory & Aiken, 1993; De Weerd, Desimone & Ungerleider, 1998; Hsu, Yeh & Kramer, 2006), (B) receptive field (RF) changes (Júnior, Rosa, Gattass & Rocha-Miranda, 1992; Pettet & Gilbert, 1992; DeAngelis, Anzai, Ohzawa & Freeman, 1995), (C) cortical topographical map reorganization (Recanzone, Merzenich & Dinse, 1992), and (D) neural adaptation or fatigue (De Weerd, Gattass, Desimone & Ungerleider, 1995; Weil, Kilner, Haynes & Rees, 2007). The available literature on artificial

scotoma reviewed here indicated that most of the stimulus features that render a target invisible are in fact engaging, or preferentially processed by, the magnocellular (M) pathway. For example, the time taken for an achromatic target region to fade in an artificial scotoma paradigm depends on the eccentricity and size of the target (De Weerd et al., 1998). In contrast to the boundary adaptation account, their results can also be explained by the fact that there are more magnocellular afferents (mostly achromatic and large RF) in the periphery than in the fovea (Croner & Kaplan, 1995). The experiments described here examined how stimulus attributes that are preferentially processed by the magnocellular pathway affect the time taken to induce a scotoma. This study may also help inform us about why similar stimulus parameters affect the process of filling-in in the related phenomenon of motion-induced blindness (MIB). Hsu et al., (2006) demonstrated that the same mechanisms are likely to be responsible for the disappearance of targets in artificial scotoma and motion induced blindness. The relationship between M channel activity and artificial scotoma would further inform us about perceptual filling-in processes.

The next section, reviews the current state of our understanding of the behavioral and physiological characteristics of the M (magnocellular) and P (parvocellular) streams. In addition to the M and P pathways, the K (koniocellular) pathway constitutes the third visual pathway in primate lateral geniculate nucleus (LGN). It is comprised of small cell bodies, which lie interlaced between the main laminae in a diffused manner (Hendry & Reid, 2000). The koniocellular (K) channel is anatomically and physiologically distinct from the M and P pathways, and innervates significantly fewer neurons (approx. less than 10%) as compared to the other two pathways (Kaplan, 2004). Researchers discovered the presence of K pathway in primates only in the last few decades and very little is known about the K pathway contribution

to human vision. Recent studies have found that many cells in the koniocellular division carry short wavelength information, which has led to the belief that the K neurons are involved in blue/yellow chromatic processing (Martin, White, Goodchild, Wilder & Sefton, 1997). In addition, K cells are heterogeneous in their RF size and spatio-temporal response to visual stimuli compared to M or P cell (Xu et al., 2001). Thus, it is likely that the koinocellular pathway has little, if any role in inducing an artificial scotoma.

M and P Pathways

Our visual system is composed of several neuronal groups that are coarsely performing different visual functions. The distinctions between the M and P neurons are based on important dimensions such as morphology, physiology, and connectivity. Polyak (1941) was the first to describe two major types of ganglion cells namely the midget and the parasol cells. The midget cells constitute the P pathway and the parasol cells constitute the M pathway (Boycott & Wässle, 1991; Calkins & Sterling, 1999). Primate studies established the existence of the direct projection of the parasol cells to the magnocellular layers of the LGN i.e., the bottom two layers, whereas the midget ganglion cells project to the four upper layers, which are the parvocellular layers (Leventhal, Rodieck & Dreher, 1981; Perry, Oehler & Cowey, 1984). The magnocellular cells synapse in layer 4Ca and parvocellular cells synapse in 4Cb in the striate cortex. Information is relayed from V1 to the rest of the visual system.

There are several physiological differences in the organization of the M and P streams in the visual system. The study of the dendritic field size at two retinal eccentricities suggests that the P to M ratio in the central retina might be as high as 30 to1 indicating differences in the distribution density of M and P cells in the retina (Dacey & Petersen, 1992). Additionally, the diameter of receptive field size increases for both M and P cells with increasing eccentricity, but

the RF diameters of the M cell's receptive fields increases much more than those of the P cells at the same retinal eccentricity (Croner & Kaplan, 1995). These RF characteristics have consequences for the cell's contrast sensitivity, spatial resolution, chromatic selectivity, as well as their state of light adaptation.

Response Characteristics

Gouras (1968) was the first to report that there were two responses to light steps; some cells responded in a tonic or sustained fashion, whereas others responded phasically. This difference is one of the clearest distinguishing characteristics of M and P cells. The time course of the neural response of the M and P cells have also been described in terms of transient and sustained, dual channel perspective. The M-cells have a fast or transient response to onsets whereas the P-cells have a slower tonic or sustained response to stimulus onsets. Breitmeyer and Ogmen (2006) have reviewed psychophysical data indicating that the transient and sustained channels have response properties consistent with the M and P pathways.

The M cells have higher contrast gain for luminance patterns at low contrasts whereas the P cells have low contrast gain for all contrasts (Kaplan & Shapley, 1986). Like contrast gain, the M cells are more light adapted and therefore more transient than P cells at any given luminance level. Since the RF size affects how many photons are collected by a given cell (Enroth-Cugell & Shapley, 1973), the difference in RF size of M and P cells is thought to modulate their contrast gain, spatial resolution, and light adaptation (Croner & Kaplan, 1995). The M and P populations also differ in their chromatic selectivity (Gouras, 1968). Most P cells demonstrate spectral selectivity and antagonism, whereas the selectivity of the M population is more broadband (Hubel & Wiesel, 1968). However, this does not imply that M cells do not analyze any chromatic information (Derrington, Krauskopf & Lennie, 1984). It is also important to note that the M and

P systems are not uniform or completely independent neuronal populations as might be suggested by the notion of parallel systems or streams popularized by lesion studies (Livingstone & Hubel, 1988; Hegde & Felleman, 2007).

This clustering of anatomical and physiological properties of the M and P cells has led to the grouping of their functional properties. The parvocellular system is thought to participate in processing form and color since its cells are characterized with small receptive fields and chromatic sensitivity. On the other hand, the magnocellular system specializes in detecting motion and conveying information about luminance. These differences between M and P pathways can be used to manipulate and bias the relative contribution of either pathway to different visual phenomenon. Examples of such manipulations in the literature include: using spatial frequency defined stimuli to take advantage of differences in spatial resolution of the M and P pathway (Breitmeyer & Ganz, 1976; Livingstone & Hubel, 1988; Brown, 2009), using equiluminant stimuli to reduce the contribution of the M system (Cheng, Eysel, & Vidyasagar, 2004), using the steady and pulsed pedestal (S/PP) paradigm to take advantage of luminance contrast gain differences in the M and P pathway (Pokorny & Smith, 1997), and using different temporal frequencies (Merigan, Byrne & Maunsell, 1991).

Artificial Scotoma

In 1991, Ramachandran and Gregory published a novel technique to generate an artificial scotoma. In a typical perceptual scotoma paradigm, a peripheral grey square target is presented on a dynamic achromatic noise background of matched luminance (see Figure 1). As the participant fixates on the center of the display, the target is filled-in by the background and then reappears over time or as soon as an eye movement is made. They used a homogenous grey square target, subtending 1.5° visual angle placed 6° in the periphery, overlaid on a background

of twinkling noise of the same mean luminance for 10 seconds of steady fixation. The background of the display subtended 19° x 15° visual angle, flickering at 10Hz or 30Hz with a luminance of 25 cd/m^2. All the participants reported fading of the grey square target within the first few seconds of the stimulus onset. This phenomenon mimics the phenomenological experience of a pathological scotoma or a blind spot.

Literature examining perceptual filling-in mechanisms that underlie pathological scotoma and blind spots is extensive. Typically, these studies use relatively small targets placed outside the scotoma region such as the ends of a bar on the opposite sides of the blind spot. These targets are often reported as a completed object (in this case, a single bar) occupying the physically blank space between the ends. Although this form of perceptual completion is similar to the filling-in of an artificial scotoma, it is important to note a few differences. First, a pathological scotoma can be located in the foveal region whereas artificial scotomas are generally in the periphery (i.e., only stabilized images can induce a foveal scotomas). In comparison, the retinal location of a blind spot is relatively similar and permanent in all participants. Second, the blind spot is present from birth and a pathological scotoma may be present in the visual system for either several weeks or years from their onset. An artificial scotoma, on the other hand, is only present in the visual system for a few seconds. This is important because any receptive field changes and/or cortical reorganization associated with each individual manifestation of these may not be comparable. Third, the area and shape of the scotoma is variable in each manifestation. For instance, the natural blind spot usually occupies much smaller area as compared to artificial or pathological scotomas. Thus, this chapter has been limited to reviewing and examining the literature on perceptual filling-in of scotoma inducing visual displays.

Regardless of these differences, there seems to be minimal behavioral differences in perceptual filling-in latencies for lesioned and intact retinal regions. Alvarenga, Couto, and Pessoa (2007) compared the filling-in process between lesioned retinas and preserved retinas in the same eye for patients with monocular toxoplasmic retinochoroiditis scotoma. They recruited thirteen participants between the ages of 18 to 66 years with intact foveas and good visual acuity. They tested the time taken for filling-in using Ramachandran's artificial scotoma paradigm (1991) for both the scarred and the healthy regions at the same eccentricity from the fovea. The average scar size was 10° located with 30° outside the fovea. There were no significant differences between the lesion and intact retinal regions. Crossland and Bex (2009) reported similar results when they tested the spatial alignment efficiency of pathological scotomas and blind spots with line or bar stimuli that either were abutting the edge of the blind spot or placed right next to it. The spatial alignment thresholds for the blind spot and the pathological retinal regions were dependent on the placement of the bar and not on the type of scotoma. Although the above stated studies indicate that blind spots, artificial and retinal scotomas are behaviorally similar, the filling-in at blind spots and retinal scotoma are not as affected by specific stimulus parameters like color, equiluminant target and background. The next section describes specific factors that affect the time taken for a target to fade in an artificial scotoma paradigm in addition to summarizing the previously proposed accounts to explain why the peripheral target disappears when placed on a random dot background.

Boundary adaptation

Boundary adaptation was one of the earliest explanations for the occurrence of artificial scotoma. Ramachandran and Gregory (1991) were the first to test whether adaptation was causing the fading of the target. They switched off the square target after it perceptually

disappeared and replaced it with a smaller concentric square. The offset transient did not help the reappearance of the target but the onset of the smaller square rendered the smaller square visible. The smaller square filled-in again within a few seconds. They also reported that the amount of displacement necessary for restoring the visibility of the target was dependent on the target eccentricity (Ramachandran, Gregory, & Aiken, 1993). Taken together, these two studies demonstrate that neural adaptation at the boundary of the target was responsible for the target's disappearance (since the target displacement rendered it visible rather than its offset).

Ramachandran and colleagues (1993) reported longer fading times for static random dot images as compared to dynamic random dots. They attributed neural fatigue of detectors that are specialized in extracting texture or kinetic edges as a casual factor for the differences in fading time for static and dynamic images. For each trial, participants adapted to the display for 20 seconds. After the display offset, the participants reported viewing an afterimage with twinkling noise only at the target location and not in the surround region. The presence of these afterimages implied an active neural representation of the invisible target in the scotoma region as opposed to the proposition that faded targets tend to be ignored. A target placed within the fovea creates a similar afterimage after switching off the twinkling background (Tyler & Hardage, 1998). This effect occurs after prolonged adaptation to the background, and is referred to as twinkle aftereffect. The implications of this study are discussed later on.

De Weerd et al., (1998) demonstrated robust evidence for the role of boundary adaptation in an artificial scotoma. They displaced the target in upward, downward, left, and right directions of displacement by 0° to 1.6° every 1 second after the target disappeared during each trial. Only 0.2° of target displacement was sufficient to increase the time taken to fill-in the target significantly. Targets did not fill-in at any other larger displacements. After the target is filled-in,

any large displacement will produce a new, noticeably bigger transient M response thereby disrupting the filling-in process. The large transient has an effect comparable to when an eye-movement is made after the target is filled-in. Displacing the background in the same manner had no such effect, supporting the idea that boundary adaptation also plays an important role in the filling-in process.

Reduction in neural activation

De Weerd et al., (1995) proposed that the boundary adaptation account is complimentary to changes in neural activity during the process of filling-in of an artificial scotoma. They compared the time taken for the filling-in process for both humans and rhesus monkeys while they were observing the same stimuli. The stimulus was a texture background consisting of randomly placed bars (size of 0.2° x 1.4°) and a target 'hole' of equal luminance to the background. At an eccentricity of 8°, the time taken to fill-in the hole increased as the size of hole increased from 1° to 12.8°. The rhesus monkey's neural response was marked by significant lowering of firing rates when the target faded for the 'hole' condition as compared to the 'no-hole' condition with no target. However, after a few seconds, for the 'hole' region the activity gradually increased to a comparable level as if the texture with the hole was the same as the texture without the hole. The authors termed this gradual neural firing increase as "climbing activity". The time course of climbing activity for primates was comparable to the time taken by human participants to report filling-in. They also found that the initial transient response to the 'hole' size of 5.6° or bigger was lower which caused the reduction in initial activity. This in turn increased the time taken for the climbing activity or filling-in to occur. The smaller texture surround background (4.4° x 4.4°) for small 'hole' size (< 4°) showed significantly reduced climbing activity suggesting that the 'hole' boundary *per se* did not affect the climbing activity

or the filling-in, rather that the surrounding context matters. They proposed that neural adaptation caused the lowering of neural inhibition, which meant that neurons had lowered levels of excitation to climb over time. They argued that long-range horizontal connections and feedback loops mediated these relative inhibitory and excitatory processes.

Weil et al., (2007) used frequency tagged MEG response to study the neural basis of filling-in of an artificial scotoma. They used a flickering uniform target at 7.5 Hz and measured steady-state responses specific to this stimulus frequency. Flickering target only allowed for the study of stimulus-related signal changes associated with perceptual completion. The recorded signals were sensitive to the target and its corresponding retinotopic location and not the background. Like De Weerd et al., (1995) they also found a significant reduction in MEG response when the target was filled-in as compared to target-visible epochs. The MEG response to the target-absent condition was significantly lower than the invisible epoch. The authors argued that the reduction in response for a persistent target specific representation indicated that both the invisible target and the perceptually completed background might be represented at the same retinotopic location.

In another study, Weil, Watkins, and Rees (2008) used functional MRI to locate specific regions with reduced activity in the cortex associated with perceptual completion of an artificial scotoma. They measured reductions in activity for the retinotopic representation of the target in primary visual cortex areas V1 and V2 of human participants. Their results verified that the filling-in of an artificial scotoma was associated with significant reductions in the BOLD activity for both retinotopic regions, and this reduction was higher than the activity recorded when the target was physically absent. Interestingly, they also recorded some reduction in activity for distal background stimuli in V1. This provides further support for contextual effects in artificial

scotomas (De Weerd et al., 1995; De Weerd et al., 1998). This persistence of neural signals associated with the target, even after perceptual completion might indicate the presence of a persistent neural representation of the invisible target.

Receptive field changes and spread of activation

Sensory learning has considerable impact on neural plasticity in the cortex (Weinberger, 1995; Buonomano & Merzenich, 1998). In comparison to the higher sensory and subcortical areas, the role of learning based plasticity in sensory cortical plasticity is not well understood. Strong evidence for sensory cortical remapping in humans comes from the large-scale receptive field reorganization of somatosensory and motor cortical areas in the weeks or months immediately following limb amputation (Fuhr et al., 1992; Knecht et al., 1995). To test training dependent plasticity, Recanzone et al., (1992) trained monkeys to discriminate between different frequencies of successive vibratory stimuli. Over time, receptive fields representing the trained skin enlarged several-fold in these monkeys. Bakin and Weinberger (1990) observed similar results in the primary auditory cortex.

In contrast to the strong evidence of RF plasticity in the somatosensory and auditory cortices, the evidence for plasticity in the visual cortex is less certain. In a striate cortex deprivation study, Gilbert and Wiesel (1992) observed increases in receptive field size of cortical cells near the edge of the artificial scotoma. They mapped receptive field changes by recording single cell activity of 53 neurons in V1 to the occluded or masked retinal region of a cat. They created a masked visual space by excluding the moving bars from the region corresponding to the RF of the neurons that were recorded. This masked space in their experimental display represented an artificial scotoma. The results demonstrated a fivefold increase in RF size following the masked conditions. However, they observed little expansion for a blank screen

indicating the importance of stimulation of surround regions. The authors argued that their results support the idea that the plastic and dynamic nature of RF's could account for perceptual filling-in. However, DeAngelis et al., (1995) were unable to replicate the results of the Pettet and Gilbert (1992) study when they used a similar experimental procedure. Instead, they found dynamic changes in response gain but no changes in the size or structure of the cortical RF of the cat. The authors suggested that the adaptation of inhibitory inputs from regions outside the classical RF caused the filling-in and not the increase in the size of RF.

Lesion studies provide stronger support for a RF plasticity account of perceptual filling-in. Júnior et al., (1992) studied the center-surround changes of receptive fields in a Cebus monkey's striate cortex for the blind spot and an artificial scotoma. They measured activity from 165 neurons in V1 during different mask conditions where they physically occluded the region covering the RF of interest. Their results indicate that the stimuli spanning beyond the boundary of the blind region for both the blind spot and artificial scotoma were completed. They also compared neural activation for bars extending over the blind spot region and the mask at different eccentricities. The neural activity for the blind spot in both the ipsilateral and contralateral eye continued in the presence of a mask as large as 10° of visual angle. Their experiment provided evidence for both the presence of RF changes and the effect of surround regions (from neurons up to 20° of eccentricity) in the perceptual filling-in process. Several other studies have demonstrated similar results suggesting that cortical neurons readjust their receptive fields in lesioned portions of the retina within a few weeks (Kaas et al., 1990; Chino et al., 1992; and Schmid, Rosa, Calford, & Ambler, 1996). They were also able to demonstrate inactivity of the lateral geniculate nucleus corresponding to the scotoma for two months after the retina was lesioned.

Stimulus parameters

De Weerd, Desimone, and Ungerleider (1998) were the first to conduct a comprehensive parametric study of filling-in using the artificial scotoma paradigm. They varied several stimulus attributes like the target size, stability, eccentricity, shape and the relative surrounding texture size to study their effects on the filling-in process. The stimulus background used was a dynamic texture made of jittering horizontal line segments with an equiluminant target. There was a steady increase in time required for filling-in from about 3 seconds to about 10 seconds as the target sizes increased from 0.6° to 5.6° at an eccentricity of 8°. The authors suggested that the inhibitory antagonistic surrounds of larger targets took longer to adapt, hence increasing the time taken to fill-in.

Next, De Weerd et al., (1998) tested the smallest size of the surround required for filling-in to occur in order to see how the spatial extent of the background interacts with the filling-in process. They used four different target sizes (1°, 2°, 4° or 6°) presented at an eccentricity of 8° within eight texture backgrounds of widths ranging from 0.1° to 8°. The time required to fill-in decreased as the background size increased contingent on the target size. Filling-in did not occur for a 6° target within a 0.4° background frame. When a similar frame size was used in the blind spot study, the small frame width was sufficient for filling-in to occur (Crossland & Bex, 2009). However, a small background frame did not induce an artificial scotoma. This might reflect the differences in RF expansion around a blind spot and artificial scotoma. Interestingly, on trials with a narrow texture frame, they observed filling-out of the relatively large targets suggesting a bidirectional competitive nature of the target and surround relationship.

They also tested the interaction between target size and eccentricity of the target for filling-in. Targets ranging in size from 0.1° to 7° presented at eccentricities of 2, 4, 6, 8, 12 and

20°. Participants often did not register targets placed beyond 12°, which then necessitated the use of a more salient, easily seen red equiluminant target to address the issue. The results suggested that at small eccentricities only small targets were filled-in and at a large eccentricity of 20°, targets as big as 7° were filled-in. The time required to perceive filling-in increased with increasing target size at smaller eccentricities. However, at larger eccentricities, the time taken for the target to fade did not increase linearly with the increase in target sizes. These results provide support for the possible role of Magnocellular pathway. M cells have larger receptive fields outside the fovea. Thus, changing the target size at larger eccentricities should produce little difference in filling-in latencies than the relatively more P cell mediated smaller eccentricities (Croner & Kaplan, 1995).

Ramachandran and Gregory (1991) tested whether targets are filled-in at the same time for different color and texture background conditions. They created a complex display with black dots moving horizontally in front of the grey target, which was overlaid on a pink twinkling background. The pink color filled-in the grey target before the twinkle replaced the horizontally moving dots. The authors suggested that the results might indicate separate mechanisms for filling in of color and texture. It is important to note that scotomas are harder to induce for a color display irrespective of luminance level (Ramachandran & Gregory, 1991). Spillmann, Otte, Hamburger and Magnussen (2006) were able to demonstrate similar results for color and texture in a blind spot study. They mapped the blind spot region of the participant and used a customized frame of width ranging from 0.05° to 0.66°. These frames were defined by either color, a dotted pattern or vertical bars. These different types of surrounds were used to determine the minimum region required to induce filling-in. Color frames of 0.33° were sufficient to completely fill-in the blind spot whereas a 0.66° wide frame was necessary to fill-in the dot pattern frames. It is

possible that frame size differences for color and texture conditions was mediated by the difference in RF sizes of M and P cells.

Welchman and Harris (2001) investigated the role of contrast and background context in the process of filling-in of the artificial scotoma. They tested the effect of the target and background's relative luminance and motion changes on the time course of perceptual fading. They used a display composed of dynamic random noise surrounding a target that was defined either by a difference of texture (DOT) or by a difference of motion (DOM) between target and background. The target's motion contrast was defined by, A) coherently moving dots at a constant speed lower or higher than the background, B) coherently moving dots moving in a different direction (non-random motion in background), and C) when both targets and background were stationary. The luminance contrast defined targets were brighter or darker than the average luminance of the background. Like De Weerd et al., (1998) they found an effect of eccentricity and target size with DOT and DOM displays. The DOT displays took longer to fade as compared to DOM displays suggesting that different visual areas might be relatively more active during these displays. The time taken for the target to disappear was the least when the luminance and motion contrast between the targets and the background was at a minimum. The authors suggested that the pooling of luminance and motion information over a large area seemed to modulate the time to fade indicating the importance of background areas beyond the boundary of the target. In addition, the authors acknowledge the fact that the DOT stimuli might differentially activate P, and DOM might engage M cells. The M pathway is more efficient in processing low contrasts and motion as compared to the P pathway. The above reviewed studies tested various contrast levels between target and the background. The shortest time taken for

filling-in of the target occurred only for least contrast conditions. These results reinforce our hypothesis that the magnocellular pathway plays a major role in inducing an artificial scotoma.

The studies and explanations described so far overlap but do not fully explain why specific stimulus characteristics dictate the time taken for the background noise to fill-in and why it fills-in. For example, the boundary adaptation account does not explain why a larger displacement is required at greater eccentricities without talking about receptive field characteristics of the periphery. Similarly, lowering of neural activity during target invisibility does not explain why chromatic displays are harder to fill-in or do not fill-in as compared to achromatic displays. In contrast, the M and P account proposed here is parsimonious and can account for the different traits of filling-in for this phenomenon. More support for the hypothesis comes from the study of the twinkle aftereffect (Hardage & Tyler, 1995; Tyler & Hardage, 1998). A twinkle aftereffect paradigm is quite similar to the artificial scotoma paradigm. At first, a dynamic random dot background with a grey patch in the foveal region is presented for over 20 seconds during the adaptation period; observers fixate at a spot centered in the grey target. Then a uniform grey field replaces the dynamic noise background and the participants report seeing the twinkling noise aftereffect in the region occupied by the target region. Ramachandran and Gregory (1991) first reported this aftereffect and thought it indicated a neural representation for the invisible target. However, Tyler and Hardage (1998) demonstrated the role of the magnocellular pathway in the twinkle aftereffect phenomenon. They found significantly stronger aftereffects for achromatic noise especially with frame-rates faster than 10 fps (Hardage & Tyler, 1995). They tested achromatic (black and white dots) and chromatic (red and green dots) backgrounds with two dot sizes (4 or 44 min arc), different luminance contrasts, and frame rates. Observers adapted for 20 seconds for each condition and reported when the twinkle aftereffect

ceased at the test patch location. The achromatic aftereffect for larger dots was better at low contrasts (10%) as compared to smaller dot sizes. In addition, observers reported no aftereffect for chromatic dots at low luminance contrast, further supporting their hypothesis that the twinkle induction has its origin in the magnocellular pathway (Tyler & Hardage, 1998).

The three experiments described here explored the role of the M and P pathways in the artificial scotoma phenomenon using well-established manipulations of M and P activity. It is possible that M activity facilitates the mechanisms that render the target invisible in this paradigm. Thus, if the extent of engagement or activity of the M pathway was systematically influenced, it should affect the time taken for a target to fade (TTF) in the artificial scotoma paradigm. Specifically, a relatively more M-biased stimulus that strongly activated the M system should reduce the time taken to fade. On the other hand, when the P system was stimulated relatively more, the TTF was expected be significantly increased as compared to when the M system was relatively more engaged. These two complementary hypotheses were investigated in the three experiments described later. In addition to TTF, the duration a target remained invisible (duration of target invisibility or DTI) was also recorded for all three experiments. Although DTI is not a commonly used measure in this type of research, it could possibility expand our understanding of the role of M and P pathways in this phenomenon. As demonstrated by a pilot experiment (described in Appendix A), DTI was expected to provide further evidence that when the magnocellular pathway was preferentially engaged the target region does not reappear quickly. It might reflect relatively little contribution of parvocellular pathway in recovery of target region. Thus, the targets in P-biased stimuli were expected to reappear faster than the M-biased stimuli.

Three experiments tested the two hypotheses by employing stimuli specifically chosen to preferentially increase the relative engagement of either the magnocellular or the parvocellular pathway. In the first experiment, the spatial and temporal characteristics of the display were manipulated by using different spatial frequencies within a grey square target region on achromatic random dot backgrounds flickering at three temporal speeds. The spatial frequency of the targets and flicker rates of the backgrounds were expected to preferentially engage either the magnocellular or the parvocellular pathway. A low SF within the target on a fast flickering background was anticipated to fade faster than a higher SF in the target region on a stationary background. The second experiment, a red random dot background was used to reduce the magnocellular response, which would be reflected by longer TTF. The same spatial frequency targets and background flicker rates were used as in Experiment 1. A low SF in the target region on flickering grey random dot background was expected to fade faster than a high SF in the target region on stationary red random dot background. The third experiment also altered the magnocellular activity but after the target faded. A modified steady and pulsed pedestal paradigm was used to test if M and the P-bias conditions affect the time a target remained invisible. The targets were expected to remain invisible for a longer duration on the M-biased steady pedestal as compared to the P-biased pulsed pedestal.

CHAPTER 2

EXPERIMENT 1

Several studies have examined the spatial and temporal characteristics that induce the artificial scotoma effectively. Traditionally, researchers varied the target size and background texture to study spatial changes at a range of eccentricities. On the other hand, temporal changes were investigated by varying either the speeds at which a target flickers or the speeds at which the random dot background cycles (Ramachandran, 1991; De Weerd et al., 1998; Welshman & Harris, 2001; Weil et al., 2007). The aim of this experiment was to manipulate spatial and temporal characteristics of the artificial scotoma paradigm in a way that enhanced either the magnocellular or the parvocellular contribution to the processing of the target and background region.

Spatial characteristics were manipulated by using two stationary Gabor patches placed inside a grey square subtending 2° x 2°. The random dot background flickering at three different rates were used for temporal manipulation. Researchers have taken advantage of the differences in the spatial and temporal processing of the magnocellular and parvocellular pathways to study several kinds of visual processes. The magnocellular pathway is more sensitive to low spatial and high temporal frequencies as compared to the parvocellular pathway, which is more sensitive to high spatial and low temporal frequencies (Croner & Kaplan, 1995). Spatial frequency targets have been used to study the relative role of these pathways in several paradigms such as masking (Breitmeyer & Ganz, 1976), inhibition of return (Guenther & Brown, 2012), and spatial contrast

sensitivity (Leonova, Pokorny & Smith, 2003). Using specific spatial frequency patches provided an improved manipulation to test our hypothesis.

In the present study, 0.5 cpd in the target region was compared with 4 cpd in it for three flicker rates of random dot background. The most P-biased condition, 4 cpd on a static background was expected to fade slowly and the most M-biased condition, 0.5 cpd on a background flickering at 20 fps was expected to fade quickly. The 4 cpd on a flickering background and 0.5 cpd on a static background were expected to fade at intermediate durations between the most M and P-biased conditions. If engaging the parvocellular pathway slows down the process of inducing a scotoma as evidenced by increased TTF, it is also possible that P-biased stimuli would reappear faster than M-biased stimuli. Thus, targets in P-biased conditions (high SF target, low temporal speed) were likely to reappear significantly faster compared to M-biased conditions (low SF target, high temporal speed).

General Methods

This section describes the stimuli and apparatus used in the first experiment. With the exception of changes in stimulus configuration and trial sequence, Experiments 2 and 3 used the same participants, procedure, apparatus, and data collection method as described below. The methods section for Experiments 2 and 3 will specify any deviations from this section.

Participants

The required sample size was estimated by conducting a priori power analysis using the data collected in the pilot experiment. The power analysis revealed a necessary sample size of 8-9 participants. Eleven adults participated in all three experiments (4 females, age ranging between 21 to 59 years old). All participants had normal or corrected to normal vision, normal color vision (tested with Pseudo-Isochromatic plates), and were classified as right-handed

according to the Annett Handedness Scale, or were right eye dominant. Experienced participants were recruited from a pool of local colleagues and University of Georgia (UGA) personnel. Informed consent was obtained from all participants in this project, which was approved by the UGA Institutional Review Board (# STUDY00000699).

Stimuli and Apparatus

Stimulus presentation and data collection was conducted using PsychoPy 1.80.01 software (Peirce, 2007) running on a PC computer with a color LCD monitor operating at 60 Hz which subtended a visual angle of 26.7° x 17.2°. Participants sat in a dimly lit room while using a chin and forehead-rest placed at a distance of 100 cm from the monitor.

First, the right eye blind spot of each participant was mapped to create customized videos to control for eye-movements. A blue dot was placed at the nasal edge of the blind spot for each customized video and image. If the participant reported the presence of the blue dot during a trial, it would indicate that they made a large eye movement. Such eye-movements can render the filled-in targets visible in the artificial scotoma paradigm, thereby confounding the TTF and DTI data. Trials with a response indicating such eye movements were excluded from the data analysis. Participants wore an eye patch on their left eye while their blind spot was mapped and during each experiment. To map the horizontal and vertical extent of blind spot, two hundred images were created with a 0.66° diameter blue dot placed at different locations. Participants fixated on a white circle overlaid on a grey background and reported when the blue dot was partially visible or invisible. The horizontal dot position varied between 8° to 16° away from the fixation, moving 0.4° in each image and the vertical position varied 6° below the horizontal meridian, moving 0.4° at a time as well. The blue dot position closest to the nasal edge of the blind spot was used to customize the displays for each participant. This blind spot information

was used to customize displays for Experiments 2 and 3. Several blind spots studies have used this method to eliminate the trials with large eye-movements (e.g., Tripathy, Levi & Ogmen, 1996).

The display in experimental trials consisted of: one of the two spatial frequency targets, a blue dot at the blind spot region and a black fixation dot placed on achromatic random dot backgrounds flickering at either 0 fps, 10 fps or 20 fps (see Figure 2). The entire target region physically matched the background luminance and subtended 2° x 2°. The targets were placed 10° away from the fixation, either in the top right or bottom right quadrant of the display. The location of the target was varied to control for any effect of adaptation to one retinal location. The same targets were used in the Experiments 2 and 3 and the location of the target region and fixation dot remained constant for all experiments.

Square targets were created with a Gabor patch of either 0.5 cpd or 4 cpd centered in it. High spatial frequency artifacts created due to the contour between target region and the random dot background were removed by applying a clipped Gaussian blur to the edges of the target region. The blur did not change the spatial frequency content of the Gabor patch in the target area (see Figure 3). Welchman and Harris (2003) demonstrated that blurring the target edge does not affect the time taken by a target to fade in an artificial scotoma paradigm. They degraded the target boundary to determine if boundary adaptation was facilitated by reduction of edge information. They presented a blurred edge target with a random dot background flickering at 20Hz for this purpose. A luminance cosine function was applied to the target edge to vary the spatial blur between 0.33 to 1.33cpd. The time taken to fade was similar across the different levels of blur.

A MATLAB program was used to create random dot background images with 50% dark grey and 50% bright grey dots, each subtending a visual angle of 0.2°. The random dot background was made from two luminance levels of grey dots to reduce the overall luminance of the display. The average luminance of the display was 24.8 cd/m^2. This luminance level was the closest match for the maximum luminance possible for the red random dot background (23.5 cd/m^2) used in the Experiment 2. The matched luminance allowed direct comparison of data from the two experiments. The image size of 1680 x 1050 pixels was used to match the screen resolution. Ten random dot images were converted into frames that cycled at 10 or 20 fps to create eight 40-seconds long video clips in Photoshop CS6. Four different random dot images were used for the 0 fps condition.

Procedure

All combinations of the three background flicker rates, two target types, and two target locations conditions were randomly presented in a within-subjects design. At the beginning of each trial, participants fixated while viewing the display monocularly (right eye). They initiated each trial by pressing the spacebar on a computer keyboard. Participants pressed the ‘n’ key as soon as the target fully disappeared and the ‘m’ key as soon as the target reappeared. Each trial ended either as soon as the participant pressed ‘m’ or if 40 seconds had passed since the onset of the trial. The first key press measured TTF and the second key press measured the DTI in each trial. After each trial, participants reported if they saw an afterimage by pressing the ‘y’ key and they reported if they saw the blue dot during the trial by pressing the ‘b’ key. If the participant reported an afterimage, they were instructed to not start the next trial until the afterimage disappeared. If the participants reported viewing the blue dot, it indicated that they made a large eye movement and the trail was excluded from data analysis. Participants were encouraged to

take as many breaks as needed throughout the experiment and to notify the experimenter if they had any unusual visual experience. Experiment 1 was completed in two sessions after the blind spot was mapped. There were a total of 24 practice and 192 experimental trials. Each session had eight trials per condition, excluding the practice trials. On average, each participant took a total of two hours to complete both sessions. The second session was conducted no sooner than 18 hours after the first session and no later than 72 hours after the first session for each experiment.

Results

Trials where the participant reported seeing the blue dot were excluded from the analysis. The 'n' key press measured when targets faded (TTF) and the 'm' key press measured when they reappeared (DTI). If the participant pressed 'n' but did not press 'm' during a trial, the DTI was calculated by subtracting TTF from 40, the total time allowed in seconds for each trial. If only the 'm' key was pressed, the trial was excluded from the analysis. Since target location was varied to control for adaptation to a retinal location, TTF and DTI over target location were averaged for each condition. The data in Experiment 2 and 3 were treated in the same manner.

TTF and DTI data were submitted to a 3 (background flicker rate: 0 vs.10 vs. 20 fps) x 2 (SF: 0.5 cpd vs. 4 cpd) repeated measures ANOVA. The analysis of TTF data revealed a significant main effect of background speed F (2, 20) = 16.89, η^2 = 0.63, $p < 0.001$. *Post hoc* pairwise comparisons using Bonferroni correction revealed that targets faded significantly ($p <$ 0.005) faster for backgrounds flickering at 20 fps (M = 10.54, SEM = 1.32) as compared to stationary backgrounds (M = 14, SEM = 1.19). In addition, targets faded significantly faster for backgrounds flickering at 10 fps (M = 9.78, SEM = 0.8) as compared to stationary backgrounds ($p < 0.001$). Target fade time for 10 and 20 fps conditions did not differ. As predicted, flickering backgrounds were more effective in inducing a scotoma as compared to stationary background.

The two-way interaction between background flicker rate and SF in the target region was significant F (2, 20) = 4.04, η^2 = 0.29, $p < 0.05$ (see Figure 4). Planned paired samples comparisons indicated the two-way interaction was driven by substantial differences between stationary and flickering backgrounds but not the SF in the target region. 0.5 cpd faded significantly faster for backgrounds flickering at 20 fps (t (10) = 3.40, p = 0.007) and 10 fps condition (t (10) = 4.79, p = 0.001) compared to 0 fps. Similarly, 4 cpd faded significantly faster for 20 fps (t (10) = 4.97, p = 0.001) and 10 fps backgrounds (t (10) = 4.88, p = 0.001) compared to 0 fps backgrounds. Both spatial frequency target regions faded consistently faster for flickering compared to stationary backgrounds. Although the flickering backgrounds were expected to induce a scotoma faster, SF in the target region was also expected to affect TTF. The main effect spatial frequency was not significant F (1, 10) = 0.89, η^2 = 0.08, $p > 0.05$ suggesting 0.5 cpd and 4 cpd faded equally fast. The 0.5 cpd and 4 cpd Gabors were expected to preferentially stimulate the magnocellular and parvocellular pathway. The SF within the target region seems to be a weaker manipulation compared to flicker rate of the background.

The DTI data revealed a significant difference between 0.5 cpd and 4 cpd F (1, 10) = 13.84, η^2 = 0.58, $p > 0.005$ (see Figure 5) suggesting the target region was actively processed by the visual system even when it was perceptually unavailable. This is consistent with the idea that the target region is not ignored after fading as suggested by Dennett (1992), rather an active representation is possibly maintained during the time the target is invisible (Pessoa, Thompson, & Noë ,1998; Weil & Rees, 2008). Contrary to prediction, 0.5 cpd reappeared significantly faster (M = 4.03, SEM = 0.67) than 4 cpd (M = 4.99, SEM = 0.78). 0.5 cpd might have reappeared faster due to better detectability of low SF in periphery than 4 cpd. Weisstein and Wong (1986) have shown that low SF in background is detected better than high SF. They found that the

blurred low spatial frequency targets were detected better when they were flashed in ground regions than when they were flashed in figural regions and vice versa for high spatial frequency targets. The also reported that faster flickering region was perceived as ground and slow flickering regions was perceived as figure. They demonstrated low spatial frequency channels are involved in ground analysis and high spatial frequency channels are involved in figural analysis (Henning, Hertz, & Broadbent, 1975). This suggests target regions were treated differently before and after they faded into the background. It is important to remember the artificial scotoma literature has never investigated factors that affect when targets reappear. The predictions for DTI in these three experiments were speculations based on the pilot data from three participants and it is possible that the visual pathways process the target region differently before and after they fade.

Contrary to TTF, background flicker rate did not affect when the target reappeared F (2, 20) = 0.86, η^2 = 0.08, p > 0.05. Background flicker rate affected the TTF while target SF affected DTI. This suggest a dichotomy in which factor affects TTF and DTI. The background appears to be dominant factor in deciding when the target fades. Once the target fades, the characteristics within the target region appear to become influential in determining when it reappears, further supporting the role of active competition between the figure and ground regions of the display.

CHAPTER 3

EXPERIMENT 2

This experiment examined how achromatic and chromatic random dot backgrounds affect the time taken to induce a scotoma. Comparing chromatic and achromatic conditions is another technique for examining the effect of the M and P-biased stimuli in filling-in of a peripheral target. Most of the M cells do not demonstrate spectral selectivity, whereas the P cells specialize in antagonism and spectral processing (Hubel & Wiesel, 1968). Typically, researchers use equiluminant chromatic stimuli or full field red backgrounds in a task to reduce the role of the magnocellular pathway. Several perceptual tasks like global motion perception (Chapman, Hoag & Giaschi, 2004), spatial attention (Yeshurun, 2004), metacontrast masking (Breitmeyer, May & Heller 1991) and schizophrenia research (Bedwell, Brown & Miller, 2003) have used red stimuli to control or reduce magnocellular activity. Tyler and Hardage (1998) used equiluminant red-green stimuli to examine the role of the magnocellular pathway in the twinkle aftereffect paradigm. They found significant differences between achromatic and chromatic conditions, with chromatic backgrounds almost eliminating the aftereffect. Ramachandran (1991) used an equiluminant pink background and grey target to test the differences in color and texture processing in the filling-in of an artificial scotoma. They reported that the pink color filled-in the grey target before the twinkle replaced the horizontally moving black dots suggesting difference in the time course for filling-in of color and texture. However, a full field red random dot background has not been used in the artificial scotoma paradigm. This experiment utilized a random dot background made from two luminance levels of red dots to reduce the M response.

In the present study, 0.5 cpd was compared with 4 cpd for two flicker rates of red random dot background and grey random dot background (Experiment1). The most P-biased condition, 4 cpd in the target region on a static red background was expected to fade slowly and the most M-biased condition, 0.5 cpd on a grey background flickering at 20 fps was expected to fade quickly. 4 cpd on 20 fps flickering grey background and 0.5 cpd on static red background were expected to fade at intermediate durations between the most M and P-biased conditions. For DTI, it was hypothesized that the targets in the most P-biased conditions (high SF target, 0 fps red background) would reappear significantly faster compared to the most M-biased conditions (low SF target, 20 fps grey background). In addition, the number of trials where targets do not disappear were expected to be much higher for the red compared to the grey background condition (Ramachandran, 1991).

Methods

Stimuli and Apparatus

Stimuli presentation and data collection was conducted in the same manner as described in Experiment 1. The display consisted of spatial frequency in the target region, a blue dot at the blind spot region, a black fixation dot placed on a red random noise backgrounds flickering at 0 or 20 fps. The blind spot position observed in Experiment 1 was used to customize the chromatic displays. The background images were created with MATLAB program to create random dots of two levels of red luminance. The average luminance of the bright and dark red dots was 23.5 cd/m^2 (maximum). This was the closest match to the average luminance of 24.8 cd/m^2 used in Experiments 1 which allowed for the direct comparison of the data from Experiments 1 and 2. Five images were converted into frames that cycled at the speed of 20 fps to create four-40 seconds long videos for each participant using Photoshop CS6. The four images used for the 0

fps condition were different from the images used to create the videos (see Figure 6). The 0 and 20 fps condition data from the first experiment was added as the achromatic condition trials. The SF targets regions created in Experiment 1 were used in this experiment with no change to their location, size, or luminance.

Procedure

The procedure was the same as in Experiment 1 with the exception of eliminating 10 fps condition. The data was collected in two sessions lasting one hour each. There were a total of 16 practice and 128 experimental trials split equally between the two sessions. The TTF and DTI were recorded in the same manner as in Experiment 1.

Results

Preliminary analysis revealed that on average, participants did not see the target fade in at least 30% of the trials for all conditions (M = 34.3%, SEM = 6.7%). There were individual differences in how often a target faded for each participant (see Figure 8). Some participants did not see the target fade for 56.75% of the trials on average (n = 4, SD = 16.72%). Other participants saw the targets fade for 91.1 % of trials (n = 4, SD = 6.09%). Thus, TTF and especially DTI data was inadequate for statistical analysis. To better understand the difference between the different conditions, the data was recoded. Trials where targets faded were assigned a ‘0’ and trials without a fade response were assigned ‘1’. A ratio of trials without fade response to total number trials per condition was computed for each participant.

This measure was submitted to a 2 (background color: red vs. grey) x 2 (background flicker rate: 0 vs. 20 fps) x 2 (SF: 0.5 cpd vs. 4 cpd) repeated measures ANOVA. Consistent with the prediction, analysis of this ratio revealed a significant main effect of background color F (1, 10) = 25.46, η^2 = 0.72, $p < 0.005$ suggesting scotomas were induced more readily for grey than

red random dot backgrounds (see Figure 7). Participants consistently reported more difficulty in perceiving the target region fade during trials with red background compared to grey backgrounds (Experiment 1). Targets faded more often for both grey and red flickering backgrounds as compared to static red and grey backgrounds F (1, 10) = 9.52, η^2 = 0.49, p < 0.05. The main effect of target SF was not significant F (1, 10) = 0.49, η^2 = 0.05, p > 0.05 suggesting background color and not the SF in the target region caused the reduction in number of times targets faded.

Planned comparisons demonstrated the significant two-way interaction between background color and flicker rate F (1, 10) = 4.96, η^2 = 0.33, p < 0.05 was caused by pronounced ease of fading for grey background. The target region faded significantly more often on grey background than red backgrounds for both 20 fps condition t (10) = 3.37, p = 0.007 and 0 fps conditions t (10) = 5.16, p < 0.001. Flickering red backgrounds facilitated fading more than stationary red backgrounds t (10) = 2.8, p = 0.01. The flickering and static achromatic backgrounds facilitated fading of target regions equally. These results indicate that achromatic backgrounds were most effective in inducing a scotoma while red stationary backgrounds were the least effective. These results are consistent with the prediction that targets on M-biased grey flickering background should fade more than targets on P-biased red stationary background.

CHAPTER 4

EXPERIMENT 3

Artificial scotoma studies have shown that the contrast between target regions and their backgrounds affects the time to fade. The contrast between target and backgrounds can be motion defined, luminance defined, motion direction defined, or color defined. The time taken for a target to fade is the smallest at zero contrast between target and background. This is true for all types of contrasts between target and background (Welchman & Harris, 2001; De Weerd et al., 1998). It is also well known that the magnocellular system is much better at detecting low luminance contrasts compared to the parvocellular system (Kaplan & Shapley, 1986). The aim of the present experiment was to study the artificial scotoma paradigm by taking advantage of known differences in luminance contrast processing of the magnocellular and parvocellular pathways. The steady and pulsed pedestal paradigm is one established method for examining the contrast related response of the M and P pathway (Leonova, et al., 2003; Pokorny & Smith, 1997; Smith & Pokorny, 2003). This paradigm has been shown to successfully bias the M and P pathways for contrast sensitivity research with spatial resolution (Leonova et al., 2003), aging (Elliott & Werner, 2010), retinitis pigmentosa (Alexander, Barnes & Fishman, 2003), glaucoma (McKendrick, Badcock & Morgan, 2004), amblyopia (Zele, Pokorny, Lee & Ireland, 2007), and schizophrenia (Delord et al., 2006).

There are two main conditions in this paradigm; the steady pedestal and pulsed pedestal condition (Pokorny & Smith, 1997). In the steady pedestal condition, stimuli are presented on a luminance pedestal, which is a region of space with a luminance value different from the

background. This pedestal is displayed for the entire duration of the trial. The target appears for a short duration and the magnocellular pathway is thought to mediate processing in this condition. The pulsed pedestal condition has a luminance pedestal that appears briefly with the onset of the target stimulus. The large transient onset of the luminance pedestal is thought to overstimulate and then reduce the activity in magnocellular pathway thereby biasing the P system for this condition (Leonova, et al., 2003). In several studies, the pedestal position and size were modified in different ways and produced consistent results in each modification. Pokorny (2011) has reviewed the various adaptations and implications of the steady and pulsed pedestal paradigm.

In the current experiment, the steady and pulsed pedestal paradigm was modified to incorporate traditional artificial scotoma stimuli. Instead of the traditional pedestal configuration, the random dot background acted as a fixed central region and a grey surround became the pedestal. Introducing a luminance pulse to the surround should not be expected to affect the reappearance of the faded target region as participants were asked to ignore the onset while fixating. The steady pedestal had no luminance change in the surrounding pedestal while the participants made the TTF and DTI responses. In the pulsed pedestal condition, the luminance of the grey surround changed from dark to bright grey 250 milliseconds after the target faded. This type of surround luminance pulse has been effectively used for temporarily reducing magnocellular activity in inhibition of return (IOR) and object advantage studies (Guenther, 2011). Reduction in the size of the random dot background in this experiment was not expected to limit the effectiveness of random dot display in inducing a scotoma. De Weerd et al., (1998) reported that a much smaller background size was effective in inducing a scotoma as long as the target size was proportionally reduced.

In this experiment, the magnocellular activity was altered after the target faded. Target regions with 0.5 cpd and 4 cpd in them were compared for both pedestal conditions. The most P-biased condition of 4 cpd on a pulsed pedestal was expected to fade slowest and the most M-biased condition of 0.5 cpd on steady pedestal was expected to fade quickest. 4 cpd on steady pedestal and 0.5 cpd on pulsed pedestal were expected to fade and reappear at intermediate durations. For DTI, the targets in the most P-biased conditions (4 cpd, pulsed pedestal) were expected to reappear significantly faster than the most M-biased conditions (0.5 cpd, steady pedestal). Introducing the pulse after the target faded was used to create an M-bias after the target faded.

Methods

Participants

Same as described in Experiment 1 with the exception of an additional participant. Twelve adults participated in this study (5 females and 7 males; age ranging between 21 to 59 years old).

Stimuli and Apparatus

Stimuli presentation and data collection was conducted in the same manner as described in Experiment 1. The blind spot position obtained in Experiment 1 was used to customize the pedestal displays. The display consisted of spatial frequency targets, a blue dot at the blind spot region, and a black fixation dot placed on random noise central region, which was surrounded by a grey homogenous background. The background images were created with a MATLAB program that changed the size of the central random dot region to 1488 x 888 pixels while keeping the display size constant by adding a grey surround subtending 2°. Two levels of grey surround luminance were used 10 cd/m^2 and 55 cd/m^2. The average luminance of the random dot

central region of the display remained unchanged. The targets created in Experiment 1 were used in this experiment with no change to their size, SF, luminance or location in the display. Eight images were created for each participant using Photoshop CS6.

Procedure

Every combination of two background pedestals, two target types, and two target locations were randomly presented in a within-subjects design. The procedure was the same as Experiment 1 with the exception that all trials were presented with stationary backgrounds. The participants initiated each trial by pressing the spacebar on a computer keyboard. In the steady pedestal condition, a bright grey surround pedestal was present while the participants pressed the 'n' and the 'm' key to indicate when a target faded (TTF) and when it reappeared (DTI). In the pulsed pedestal condition, a dark grey surround pedestal was present until 250 msec after the target faded followed by the onset of the bright grey surround pedestal, which lasted until they pressed the 'm' key to indicate that the target reappeared or 40 seconds had passed since the onset of the trial (see Figure 9). Participants were asked to report viewing any afterimage or the blue dot in the same manner as described in general methods section. Like the previous experiments, data was collected in two sessions that lasted 45 minutes each. There were a total of 16 practice and 128 experimental trials split equally in each session.

Results

The TTF and DTI were recorded in the same manner as in Experiment 1. The TTF and DTI data was submitted to a 2 (pedestal type: steady vs. pulsed) x 2 (SF: 0.5 cpd vs. 4 cpd) repeated measures ANOVA. In addition, the steady and pedestal conditions were compared with static achromatic conditions from the first experiment to rule out effect of reduced random dot region or the luminance pedestals.

The results show the time to fade differed significantly for the two pedestal conditions F (1, 10) = 30.95, η^2 = 0.74, $p < 0.001$; neither steady nor pulsed pedestal differed from the static random dot condition from Experiment 1 (see Figure 10). It is likely the steady and pulsed pedestal conditions were associated with significantly different fade times due to a difference in the overall luminance of the display. The targets on pulsed pedestal faded quickest (M = 13.39, SEM = 1.24) followed by the static condition from Experiment 1(M = 13.89, SEM = 1.15) and the slowest for the steady pedestal condition (M = 15.31, SEM = 1.12). The is consistent with the combined overall luminance of random dot central region and the pedestal surround for each display. The pulsed pedestal had the least (23.05 cd/m^2) and steady pedestal had the highest (29.25 cd/m^2) combined luminance. These results indicate pooling of surround spatial information. Some studies have indicated the role of both immediate and distant surrounds in fading of targets (De Weerd et al., 1995; Weil et al., 2008). Contrary to prediction, 4 cpd faded significantly faster than 0.5cpd for both steady and pulsed pedestals. It is unlikely the overall luminance of the pedestals created this affect because the SF's on static backgrounds showed a similar trend t (10) = 3.37, p = 0.08 (Experiment 1).

Although surround luminance pedestal affected TTF, it is not likely to affect DTI since the overall luminance for both pedestals was the same after target faded. This was also confirmed by the fact that DTI for full random dot background from Experiment1 was similar to DTI for steady pedestal (t (10) =0.31, p = 0.84) and not pulsed pedestal condition (t (10) = 2.54, $p <$ 0.05). If surround luminance were to affect DTI, both pulsed and steady pedestal conditions should have similar reappear times that were different from full grey random background. These results demonstrate that the luminance pulse onset and not the surround luminance affected DTI.

Analysis of DTI revealed a significant main effect of pedestal F (1, 11) = 22.3, η^2 = 0.67, $p < 0.001$ (see Figure 11). The results demonstrate that targets reappeared faster for the P-biased pulsed condition (M = 2.89 sec) as compared to M-biased steady pedestal condition (M = 4.33 sec). Contrary to prediction, the M-biased 0.5 cpd targets (M = 3.16 sec) reappeared consistently faster than P-biased 4 cpd targets (M = 4.07 sec) for both pedestal conditions F (1, 11) = 18.9, η^2 = 0.63, p = 0.001. These results are consistent with the results from Experiment 1 where 0.5 cpd reappeared faster than 4 cpd for static full random dot backgrounds. This supports the idea that loss of figure status after fading changes the way target region is processed during its recovery. This is consistent with the prediction that the magnocellular pathway affects fading and reappearing of targets in scotomas. This further supports the possibility that the SF within the target region reliably affects when it reappears compared to the flicker rate of the background, which consistently affects the time taken to fade.

CHAPTER 6

GENERAL DISCUSSION

Even with the decline in visual acuity outside the fovea, our perceptual experience remains remarkably vivid. Filling-in mechanisms mediate this vivid phenomenological experience. Perceptual filling-in of this kind requires interpolation of surround information for completion of missing information. Fast interpolation processes contribute to filling-in of surfaces by their backgrounds during normal surface perception. Previous studies have shown that surface filling-in appears to interact with various mechanisms of figure–ground segregation (Caputo, 1996; Grossberg, 1997) and it is affected by both low-level representations of boundaries, as well as higher-level factors such as directed attention (Lamme, 1995; Peterson, & Skow-Grant, 2003). On the other hand, filling-in across artificial scotomas is a much slower process, which requires sustained viewing of a high-density noise background. It is possible that the slow perceptual filling-in mechanisms in artificial scotoma are interacting with mechanisms of figure–ground segregation. De Weerd et al., (1998) proposed that the filling-in of artificial scotoma reflects the time required for figure-ground segregation to fail as opposed to the time taken for surface filling-in. They argue that this failure is captured by the delay in filling-in of the artificial scotoma, which is opposite to the instantaneous nature of surface completion.

Previous studies have demonstrated a relationship between figure-ground segregation mechanisms and the spatio-temporal frequency channels, indicating the parvocellular pathway is actively involved in processing figure regions and the magnocellular pathway is actively involved in processing ground regions (Klymenko & Weisstein. 1986; Weisstein & Wong, 1986;

Klymenko, Weisstein, Topolski & Hsieh, 1989). This perspective is compatible with our predictions that a low spatial frequency within the target region on a flickering background should fade faster than higher spatial frequency. From a figure-ground perspective, we can describe the target region as figure on the random dot background or ground region. A low spatial frequency would lead to a weak figural response from the target region, it would compete less with the flickering background, and hence it is filled-in more quickly. On the other hand, a higher spatial frequency would lead to a stronger figural response from the target region allowing it to compete more with the flickering background leading a greater delay in fading. The results from present experiments show that this relationship between the visual pathways and figure-ground organization plays a vital role in inducing an artificial scotoma.

Three experiments were conducted to explore the role of magnocellular pathway in perceptual filling-in of an artificial scotoma. All experiment measured the time taken for a peripheral target to fade and reappear with different M-engaging or suppressing conditions. Specific spatial and temporal conditions were tested in Experiment 1, Experiment 2 utilized a red random dot background to reduce the M response, and Experiment 3 tested if task irrelevant luminance changes in the steady and pulsed pedestal conditions affected when target regions reappeared. As expected, and consistent with the literature, background flicker rate strongly affected the time taken to fade with targets on flickering backgrounds fading consistently faster than static ones in Experiments 1 and 2 (Ramachandran, 1993; Ramachandran, 1991; De Weerd et al., 1998). The goal of Experiment 3 was to introduce the pulse for DTI response to explore how M-bias influenced when the targets reappeared. TTF response was not expected to show differences due the two pedestal conditions. Contrary to this prediction, the target region on pulsed pedestals faded faster than the steady pedestals. It is likely that the steady and pulsed

pedestal conditions were associated with significantly different fade time due to difference in overall luminance of the two pedestals. The luminance of the pedestal surrounding the central random dot region did not change before or after the target faded for the steady pedestal condition (29.25 cd/m^2). However, for the pulsed pedestal condition the luminance of the pedestal surround changed from dark or low luminance to bright or high luminance 250 msec after the target faded (23.05 cd/m^2). Some studies have shown that as the luminance difference between target and backgrounds increases, fade time increases (De Weerd et al., 1998; Welchman & Harris, 2001). Others studies have demonstrated both immediate and distant surrounds can influence target fading (De Weerd et al., 1995; Weil et al., 2008). The luminance surround appears to affect the TTF differently in pulsed and steady-pedestal conditions.

The spatial frequency within the target region affected its fade time only in Experiment 3. The role of overall luminance differences in steady and pulsed pedestal displays cannot be ruled out due to the way trials were setup. The available data is insufficient for drawing meaningful conclusions. Regardless, the spatial frequency content within the target region appears to be a weak manipulation as compared to the manipulation of M-bias to the processing of the background. There are two possible explanations for these results. First, the SF within a target region occupied a very small area (2° x 2°) compared to the spatial extent of the background (26.7° x 17.2°). Targets regions are more influential in affecting the time taken to fade when there is a difference in target size, luminance or motion contrast, stability, eccentricity, and onsets (Ramachandran & Gregory, 1991; Ramachandran et al., 1993; De Weerd et al., 1998 Weil et al., 2007; Welchman & Harris, 2001). The present results indicate SF in the target region was insufficient in eliciting differences in TTF.

The difference in texture gradient between target region and the background might have contributed to the lack of SF effect on TTF. 0.5 cpd might compete more with the background due to higher texture contrast than 4 cpd. Artificial scotomas are sensitive to contrast between targets and backgrounds created due to motion, luminance, motion direction, or color (Ramachandran et al., 1993; De Weerd et al., 1998 Welchman & Harris, 2001). Welshman and Harris (2001) compared the time to fade for targets defined by luminance, motion, and motion direction. They reported equally faster fade times for horizontally moving and static dots in the target region on a random dot flickering background than a homogenous grey square target. Their result might be mediated by the increase in texture contrast between targets and backgrounds. The dots in the target region irrespective of motion would have a more similar texture gradient as opposed to the grey square target. The authors speculate that the P-bias might have increased the fade time for grey square target and the M-bias might have reduced the fade time for target defined by moving dots. It might explain why 0.5 cpd reappeared faster than 4 cpd. Experiment 3 found similar results where 0.5 cpd in the target regions reappeared faster than 4 cpd. In addition, the static conditions with 0.5 and 4 cpd in Experiment 1 were found to be similar to the DTI data for both pedestal displays in Experiment 3.

The boundary adaptation and RF expansion accounts can also explain the different fade times for background flicker rate and similar fade times for SF. These accounts attribute neural fatigue as a cause for the decrease in time taken to fade for flickering backgrounds and predict the same fade time for both SF's since the size, stability and eccentricity of target region was constant. However, these accounts cannot explain the results from Experiment 2. The red backgrounds in Experiment 2 provided the strongest support for the role of the magnocellular pathway in filling-in of the artificial scotoma. Most of the magnocellular neurons do not

demonstrate spectral selectivity, whereas the parvocellular neurons specialize in spectral processing (Hubel & Wiesel, 1968). A full field red random dot background was used to substantially reduce the M-response. Artificial scotoma studies have not used red random dot backgrounds. This experiment was designed to maximally reduce the relative magnocellular response and maximize the parvocellular response. As expected, a red random dot background significantly interrupted scotoma induction compared to grey. In addition, targets on flickering red backgrounds faded more often than static red backgrounds. Given the higher temporal frequency sensitivity of the magnocellular system (Livingstone & Hubel, 1988), a flickering background was expected to increase M-response that might facilitate fading even on a red background. The results demonstrate a substantial decrease in the percentage of trials where targets faded confirming the prediction that reducing magnocellular activity would make it harder to induce a scotoma. The red static background would constantly engage the parvocellular pathway, which has smaller RF,'s, less presence in the periphery, a sustained response, detects and discriminates high spatial frequency information better in a figure than ground region. From figure-ground perspective, the red region should be treated more as a figure than background. A static red background would compete more strongly with the target region for figure status than the grey background. Consistent with this idea, the results reflected a higher chance of fading even on static grey backgrounds than flickering red backgrounds.

The results also demonstrated large individual variance across participants in the number of times a target faded. Some participants had more difficulty seeing the target region fade than others. The individual differences in the number of times a target faded and the time taken for the target to fade were much higher for red compared to grey conditions. These differences might arise either from individual variations in the distribution of cones in the fovea and periphery

(Curcio, Sloan, Packer, Hendrickson, & Kalina, 1987; Curcio, Allen, 1990; Neitz, Neitz, & Jacobs, 1991 Wooten, & Wald, 1973) or the fact that relative numbers of long-wavelength-sensitive (L) and middle-wavelength-sensitive (M) cones vary considerably among normal trichromats (Roorda & Williams, 1999; Kremers et al, 2000). It is possible that individual differences in cone density and/or L/M ratio were reflected in the different level of difficulty experienced by participants in seeing the targets fade.

The DTI data indicated that the SF within target region affected when it reappeared rather than the flicker rate of the background. The DTI results are exactly opposite of TTF results. 0.5 cpd reappeared significantly faster than 4 cpd in both Experiments 1 and 3 and the background flicker rate had no effect on DTI in Experiment 1. In Experiment 1, neither target SF nor flicker rate changed after the target faded. However, in Experiment 3, the luminance of the surround pedestal changed from dark to bright grey after the target faded for pulsed-pedestal conditions while the steady pedestal remained unchanged throughout the trial. The steady pedestal conditions are thought to reflect M-bias while pulsed pedestal conditions are thought to reflect a P-bias (Leonova, et al., 2003; Pokorny & Smith, 1997; Smith & Pokorny, 2003). The modified pedestal paradigm was used to manipulate a task irrelevant luminance change during the DTI response for pulsed-pedestal conditions. As expected, targets in the pulsed pedestal condition reappeared faster than targets in the steady pedestal condition. Although the effect of overall luminance difference cannot be completely ruled out, it is unlikely to have influenced DTI because the overall luminance for both pedestals was equal after the target faded. DTI for a grey random dot background (Experiment 1) was similar to DTI for the steady pedestal but not the pulsed pedestal condition. If overall luminance were affecting DTI, the steady-pedestal should reappear faster than static grey, which should be similar to the pulsed-pedestal display.

Contrary to prediction, the M-biased 0.5 cpd consistently reappeared faster than P-biased 4 cpd for both pedestals. These results are consistent with the results from Experiment 1 where 0.5 cpd reappeared faster than 4 cpd for static grey backgrounds. These results indicate that target region is represented in the visual system after fading even when it is perceptually invisible. There is a large body of neurophysiological research supporting active interpolation of faded region during filling-in for artificial scotoma and surface completion (De Weerd et al., 1995; Júnior et al., 1992; Mendola et al., 2006; Pessoa et al., 1998; Pessoa & De Weerd, 2003; Weil & Rees, 2008; Weil et al., 2007; Weil et al., 2008). Our results are the first to provide behavioral data supporting this thesis for artificial scotoma.

The difference in reappearance of target regions with different SF in them can arise due to better detectability of 0.5 cpd in the periphery than 4 cpd. Previous studies have shown a low SF target in background is detected better and high SF. This might suggest that targets regions are processed differently before and after they fade due to the loss of figural status. These findings are consistent with the competitive nature of figure and ground regions of the display. Although these results are in contrast with prediction, they can still be accounted for by the M-bias created in conjunction with figure-ground organization of the display. This also explains why the SF within the target region affected when it reappeared and the flicker rate of the background affected the time taken to fade. The background seems to strongly influence when the target fades while target characteristics influence when it reappears. Traditionally, the pedestal paradigm is effective in producing biased conditions that effect reaction time and discrimination response for different visual tasks (Leonova et al., 2003; Alexander, Barnes & Fishman, 2003; McKendrick, Badcock & Morgan, 2004; Delord et al., 2006). Our results suggest that the paradigm can be adapted for tasks that do not involve speeded responses.

Taken together, the results demonstrate that altering the background characteristics by using M-engaging flicker rates (Experiment 1) and M-suppressing red (Experiment 2) and pulsed pedestal backgrounds (Experiment 3) affected delay and probability of fading while the SF within the target region affected the delay in its reappearance (Experiments 1 and 3).

Conclusions

The role of magnocellular pathway in the perceptual filling-in of artificial scotoma was examined using specific sensory manipulations. The data shows the importance of M-biased stimulus features interacting with figure-ground segregation mechanisms contributing to the artificial scotoma phenomenon. These results cast a new light on the processes mediating artificial scotoma. There are several different accounts for the time differences observed due to specific factors in artificial scotoma (Ramachandran et al., 1993; De Weerd et al., 1998; Hsu et al., 2006; Júnior et al., 1992; Pettet & Gilbert, 1992; DeAngelis et al., 1995; Recanzone et al., 1992; De Weerd et al., 1995; Weil et al., 2007). Most of these accounts can sufficiently explain why some of these factors affect this phenomenon. However, the combined magnocellular/figure-ground hypothesis based on the present experiments offers a better framework to explain challenges faced by previously proposed explanations. For example, targets had different fade times for backgrounds of different color and flicker rate. The boundary adaptation account does not explain why the color of the background would affect whether the target disappears or not. Similarly, while the RF expansion account addresses peripheral locations and background speed, it cannot explain the difference in recovery of SF regions or inability to fill-in targets on red backgrounds without including a magnocellular account. The addition of a figure-ground perspective provides a more comprehensive account for differences in the time course of fading and reappearing due to flicker rate, SF within the target region, and

the difficulty in inducing scotomas on red background. The convergence of magnocellular and figure-ground competition hypotheses seems to provide a physiologically and behaviorally sound explanation for not only the present set of experiments but for previously reported, seemingly contradictory results as well.

Additional experiments are needed to confirm whether the texture contrast or transient nature of the magnocellular pathway is affecting TTF and DTI. Further investigations controlling for overall luminance of the pedestal displays and texture gradient differences between target and background regions might help clarify the role of SF within the target region on fading and reappearance. fMRI investigation of DTI might clarify if the faded target retains its figural status unconsciously or if it blends with the background for the duration of invisibility. The present experiments also indicate a need for updating the models of filling-in to account for factors influencing DTI. Future work must thoroughly examine what happens once the target has disappeared and provide further insight into the precise mechanisms of the underlying neural processes.

REFERENCES

Alexander, K. R., Barnes, C. S., & Fishman, G. A. (2003). Deficits in temporal integration for contrast processing in retinitis pigmentosa. *Investigative Ophthalmology & Visual Science, 44,* 3163–3169.

Alvarenga, D. P., Couto, M. F., & Pessoa, V. F. (2007). Perceptual visual filling-in of toxoplasmic retinochoroiditis scotomas. *NeuroReport*, *18*(16), 1679-1681.

Bakin, J. S., & Weinberger, N. M. (1990). Classical conditioning induces CS-specific receptive field plasticity in the auditory cortex of the guinea pig. *Brain Research, 536*(1), 271-286.

Bedwell, J. S., Brown, J. M., & Miller, L. S. (2003). The magnocellular visual system and schizophrenia: what can the color red tell us? *Schizophrenia Research, 63*(3), 273-284.

Boycott, B. B., & Wässle, H. (1991). Morphological classification of bipolar cells of the primate retina. *European Journal of Neuroscience*, *3*(11), 1069-1088.

Breitmeyer, B. G., & Ganz, L. (1976). Implications of sustained and transient channels for theories of visual pattern masking, saccadic suppression, and information processing. *Psychological Review*, *83*(1).

Breitmeyer, B. G., May, J. G., & Heller, S. S. (1991). Metacontrast reveals asymmetries at red-green isoluminance. *Journal of the Optical Society of America A, 8*, 1324-1329.

Breitmeyer, B., & Ogmen, H. (2006). *Visual masking: Time slices through conscious and unconscious vision* (Vol. 41). Oxford University Press.

Brown, J. M. (2009). Visual streams and shifting attention. *Progress in Brain Research*, *176*, 47-63.

Buonomano, D. V., & Merzenich, M. M. (1998). Cortical plasticity: from synapses to maps. *Annual Review of Neuroscience, 21*(1), 149-186.

Calkins, D. J., & Sterling, P. (1999). Evidence that circuits for spatial and color vision segregate at the first retinal synapse. *Neuron*, *24*(2), 313-321.

Caputo, G. (1996). The Role of the Background: Texture Segregation and Figure—Ground Segmentation. *Vision Research, 36*(18), 2815-2826.

Chapman, C., Hoag, R., & Giaschi, D. (2004). The effect of disrupting the human magnocellular pathway on global motion perception. *Vision Research, 44*(22), 2551-2557.

Cheng, A., Eysel, U. T., & Vidyasagar, T. R. (2004). The role of the magnocellular pathway in serial deployment of visual attention. *European Journal of Neuroscience*, *20*(8), 2188-2192.

Chino, Y. M., Kaas, J. H., Smith, E. D., Langston, A. L., & Cheng, H. (1992). Rapid reorganization of cortical maps in adult cats following restricted deafferentation in retina. *Vision Research*, *32*(5), 789-796.

Croner, L. J., & Kaplan, E. (1995). Receptive fields of P and M ganglion cells across the primate retina. *Vision Research*, *35*(1), 7-24.

Crossland, M. D., & Bex, P. J. (2009). Spatial alignment over retinal scotomas. *Investigative Ophthalmology & Visual Science*, *50*(3), 1464-1469.

Curcio, C. A., Sloan, K. R., Packer, O., Hendrickson, A. E., & Kalina, R. E. (1987). Distribution of cones in human and monkey retina: individual variability and radial asymmetry. *Science*, *236*(4801), 579-582.

Curcio, C. A., & Allen, K. A. (1990). Topography of ganglion cells in human retina. Journal of *Comparative Neurology, 300*(1), 5-25.

Dacey, D. M., & Petersen, M. R. (1992). Dendritic field size and morphology of midget and parasol ganglion cells of the human retina. *Proceedings of the National Academy of Sciences, 89*(20), 9666-9670.

DeAngelis, G. C., Anzai, A., Ohzawa, I., & Freeman, R. D. (1995). Receptive field structure in the visual cortex: does selective stimulation induce plasticity? *Proceedings of the National Academy of Sciences, 92*(21), 9682-9686.

Delord, S., Ducato,M. G., Pins, D., Devinck, F., Thomas, P., Boucart, M., et al. (2006). Psychophysical assessment of magno- and parvocellular function in schizophrenia. *Visual Neuroscience, 23,* 645–650.

Dennett, D. (1992). Filling in versus finding out: A ubiquitous confusion in cognitive science. *Cognition, conception, and methodological issues.*

Derrington, A. M., Krauskopf, J., & Lennie, P. (1984). Chromatic mechanisms in lateral geniculate nucleus of macaque. *The Journal of Physiology, 357*(1), 241-265.

De Weerd, P., Gattass, R., Desimone, R., & Ungerleider, L. G. (1995). Responses of cells in monkey visual cortex during perceptual filling-in of an artificial scotoma. *Nature, 377*(6551), 731-734.

De Weerd, P., Desimone, R., & Ungerleider, L. G. (1998). Perceptual filling-in: A parametric study. *Vision Research, 38*(18), 2721-2734.

Elliott, S. L., &Werner, J. S. (2010). Age-related changes in contrast gain related to the M and P pathways. *Journal of Vision, 10*(4), 1–15.

Enroth-Cugell, C., & Shapley, R. M. (1973). Flux, not retinal illumination, is what cat retinal ganglion cells really care about. *The Journal of Physiology, 233*(2), 311-326.

Fuhr, P., Cohen, L. G., Dang, N., Findley, T. W., Haghighi, S., Oro, J., & Hallett, M. (1992). Physiological analysis of motor reorganization following lower limb amputation. *Electroencephalography and Clinical Neurophysiology/Evoked Potentials Section*, *85*(1), 53-60.

Gilbert, C. D., & Wiesel, T. N. (1992). Receptive field dynamics in adult primary visual cortex. *Nature, 356*(6365), 150-152.

Gouras, P. (1968). Identification of cone mechanisms in monkey ganglion cells. *The Journal of Physiology*, *199*(3), 533.

Grossberg, S. (1997). Cortical dynamics of three-dimensional figure-ground perception of two-dimensional pictures. *Psychological Review, 104*(3), 618-658.

Guenther, B. A. (2011). *Using the steady/pulsed-pedestal paradigm to study visual attention.* (Doctoral dissertation). Retrieved from http://purl.galileo.usg.edu/uga_etd/guenther_benjamin_a_201105_phd

Guenther, B. A., & Brown, J. M. (2012). Exploring the effect of stimulus characteristics on location-based inhibition of return using abrupt and ramped stimulus presentation. *Vision Research, 60*, 28-33.

Hardage, L., & Tyler, C. W. (1995). Induced twinkle aftereffect as a probe of dynamic visual processing mechanisms. *Vision Research*, *35*(6), 757-766.

Hegde, J., & Felleman, D. J. (2007). Reappraising the functional implications of the primate visual anatomical hierarchy. *The Neuroscientist, 13*(5), 416-421.

Henning, G. B., Hertz, B. G., & Broadbent, D. E. (1975). Some experiments bearing on the hypothesis that the visual system analyses spatial patterns in independent bands of spatial frequency. *Vision Research, 15*(8), 887-897.

Hendry, S. H., & Reid, R. C. (2000). The koniocellular pathway in primate vision. *Annual Review of Neuroscience, 23*(1), 127-153.

Hsu, L. C., Yeh, S. L., & Kramer, P. (2006). A common mechanism for perceptual filling-in and motion-induced blindness. *Vision Research*, *46*(12), 1973-1981.

Hubel, D. H., & Wiesel, T. N. (1968). Receptive fields and functional architecture of monkey striate cortex. *The Journal of Physiology*, *195*(1), 215-243.

Júnior, M. F., Rosa, M., Gattass, R., & Rocha-Miranda, C. E. (1992). Dynamic surrounds of receptive fields in primate striate cortex: a physiological basis for perceptual completion? *Proceedings of the National Academy of Sciences, 89*(18), 8547-8551.

Kaas, J. H., Krubitzer, L. A., Chino, Y. M., Langston, A. L., Polley, E. H., & Blair, N. (1990). Reorganization of retinotopic cortical maps in adult mammals after lesions of the retina. *Science*, *248*(4952), 229-231.

Kaplan, E., & Shapley, R. M. (1986). The primate retina contains two types of ganglion cells, with high and low contrast sensitivity. *Proceedings of the National Academy of Sciences*, *83*(8), 2755-2757.

Kaplan, E. (2004). The M, P and K pathways of the Primate Visual System. In L. M. Chalupa and J. S. Werner (Eds), *The Visual Neurosciences* (Vol. 1). Cambridge, MA: MIT press.

Klymenko, V., & Weisstein, N. (1986). Spatial frequency differences can determine figure-ground organization. *Journal of Experimental Psychology: Human Perception and Performance*, *12*(3), 324.

Klymenko, V., Weisstein, N., Topolski, R., & Hsieh, C. H. (1989). Spatial and temporal frequency in figure-ground organization. *Perception & psychophysics*, *45*(5), 395-403.

Knecht, S., Henningsen, H., Elbert, T., Flor, H., Höhling, C., Pantev, C., . . . Taub, E. (1995). Cortical reorganization in human amputees and mislocalization of painful stimuli to the phantom limb. *Neuroscience Letters, 201*(3), 262-264.

Kremers, J., Scholl, H. P., Knau, H., Berendschot, T. T., Usui, T., & Sharpe, L. T. (2000). L/M cone ratios in human trichromats assessed by psychophysics, electroretinography, and retinal densitometry. *JOSA A, 17*(3), 517-526.

Lamme, V. A. (1995). The neurophysiology of figure-ground segregation in primary visual cortex. *The Journal of Neuroscience, 15*(2), 1605-1615.

Leonova, A., Pokorny, J., & Smith, V. C. (2003). Spatial frequency processing in inferred PC- and MC-pathways. *Vision Research, 43*(20), 2133-2139.

Leventhal, A. G., Rodieck, R. W., & Dreher, B. (1981). Retinal ganglion cell classes in the Old World monkey: morphology and central projections. *Science*, *213*(4512), 1139-1142.

Livingstone, M., & Hubel, D. (1988). Segregation of form, color, movement, and depth: anatomy, physiology, and perception. *Science, 240*(4853), 740-749.

Martin, P. R., White, A. J., Goodchild, A. K., Wilder, H. D., & Sefton, A. E. (1997). Evidence that Blue-on Cells are Part of the Third Geniculocortical Pathway in Primates. *European Journal of Neuroscience, 9*(7), 1536-1541.

McKendrick, A. M., Badcock, D. R., & Morgan, W. H. (2004). Psychophysical measurement of neural adaptation abnormalities in magnocellular and parvocellular pathways in glaucoma. *Investigative Ophthalmology & Visual Science, 45,* 1846–1853.

Mendola, J. D., Conner, I. P., Sharma, S., Bahekar, A., & Lemieux, S. (2006). fMRI measures of perceptual filling-in in the human visual cortex. *Journal of Cognitive Neuroscience, 18*(3), 363-375.

Merigan, W. H., Byrne, C. E., & Maunsell, J. H. (1991). Does primate motion perception depend on the magnocellular pathway?. *The Journal of neuroscience, 11*(11), 3422-3429.

Neitz, M., Neitz, J., & Jacobs, G. H. (1991). Spectral tuning of pigments underlying red-green color vision. *Science, 252*(5008), 971-974.

Parkhurst, D. J., & Niebur, E. (2004). Texture contrast attracts overt visual attention in natural scenes. *European Journal of Neuroscience, 19*(3), 783-789.

Peirce, J. W. (2007). PsychoPy—psychophysics software in Python. *Journal of Neuroscience Methods, 162*(1), 8-13.

Perry, V. H., Oehler, R., & Cowey, A. (1984). Retinal ganglion cells that project to the dorsal lateral geniculate nucleus in the macaque monkey. *Neuroscience, 12*(4), 1101-1123.

Pessoa, L. E., & De Weerd, P. E. (2003). *Filling-in: From perceptual completion to cortical reorganization*: Oxford University Press.

Pessoa, L., Thompson, E., & Noë, A. (1998). Filling-in is for finding out. *Behavioral and Brain Sciences, 21*(06), 781-796.

Peterson, M. A., & Skow-Grant, E. (2003). Memory and learning in figure-ground perception. *Psychology of Learning and Motivation, 42*, 1-36.

Pettet, M. W., & Gilbert, C. D. (1992). Dynamic changes in receptive-field size in cat primary visual cortex. *Proceedings of the National Academy of Sciences, 89*(17), 8366-8370.

Pokorny, J. (2011). Review: steady and pulsed pedestals, the how and why of post-receptoral pathway separation. *Journal of Vision*, 11(5), 7.

Pokorny, J., & Smith, V. C. (1997). Psychophysical signatures associated with magnocellular and parvocellular pathway contrast gain. *Journal of the Optical Society of America A, 14*(9), 2477-2486.

Polyak, S. L., (1941). *The Retina*, Chicago: The University of Chicago Press.

Previc, F. H. (1990). Functional specialization in the lower and upper visual fields in humans: Its ecological origins and neurophysiological implications. *Behavioral & Brain Sciences, 13*, 519-575

Ramachandran, V. S., & Gregory, R. L. (1991). Perceptual filling in of artificially induced scotomas in human vision. *Nature*, *350*(6320), 699-702.

Ramachandran, V. S., Gregory, R. L., & Aiken, W. (1993). Perceptual fading of visual texture borders. *Vision Research, 33*(5), 717-721.

Recanzone, G. H., Merzenich, M. M., & Dinse, H. R. (1992). Expansion of the cortical representation of a specific skin field in primary somatosensory cortex by intracortical microstimulation. *Cerebral Cortex, 2*(3), 181-196.

Roorda, A., & Williams, D. R. (1999). The arrangement of the three cone classes in the living human eye. *Nature*, *397*(6719), 520-522.

Schmid, L. M., Rosa, M. G., Calford, M. B., & Ambler, J. S. (1996). Visuotopic reorganization in the primary visual cortex of adult cats following monocular and binocular retinal lesions. *Cerebral Cortex*, *6*(3), 388-405.

Smith, V. C., & Pokorny, J. (2003). Psychophysical correlates of Parvo-and Magnocellular function. *Normal and Defective Colour Vision*, 91-107.

Spillmann, L., Otte, T., Hamburger, K., & Magnussen, S. (2006). Perceptual filling-in from the edge of the blind spot. *Vision Research*, *46*(25), 4252-4257.

Tripathy, S. P., Levi, D. M., & Ogmen, H. (1996). Two-dot alignment across the physiological blind spot. *Vision Research, 36*(11), 1585-1596.

Tyler, C. W., & Hardage, L. (1998). Long-range twinkle induction: An achromatic rebound effect in the magnocellular processing system? *PERCEPTION-LONDON, 27*, 203-214.

Weil, R. S., Kilner, J. M., Haynes, J. D., & Rees, G. (2007). Neural correlates of perceptual filling-in of an artificial scotoma in humans. *Proceedings of the National Academy of Sciences*, *104*(12), 5211-5216.

Weil, R., Watkins, S., & Rees, G. (2008). Neural correlates of perceptual completion of an artificial scotoma in human visual cortex measured using functional MRI. *NeuroImage, 42*(4), 1519-1528.

Weinberger, N. M. (1995). Dynamic regulation of receptive fields and maps in the adult sensory cortex. *Annual Review of Neuroscience*, *18*, 129.

Weisstein, N., & Wong, E. (1986). Figure-ground organization and the spatial and temporal responses of the visual system. *Pattern Recognition by Humans and Machines: Visual Perception* (Vol. 2, pp. 31-64). Orlando: Academic Press.

Welchman, A. E., & Harris, J. M. (2001). Filling-in the details on perceptual fading. *Vision Research*, *41*(16), 2107-2117.

Welchman, A. E., & Harris, J. M. (2003). Is neural filling–in necessary to explain the perceptual completion of motion and depth information?. Proceedings of the Royal Society of London. Series B: Biological Sciences, 270(1510), 83-90.

Wooten, B. R., & Wald, G. (1973). Color-vision mechanisms in the peripheral retinas of normal and dichromatic observers. *The Journal of general physiology, 61*(2), 125-145.

Xu, X., Ichida, J. M., Allison, J. D., Boyd, J. D., Bonds, A. B., & Casagrande, V. A. (2001). A comparison of koniocellular, magnocellular and parvocellular receptive field properties in

the lateral geniculate nucleus of the owl monkey (Aotus trivirgatus). *The Journal of Physiology, 531*(1), 203-218.

Yeshurun, Y. (2004). Isoluminant stimuli and red background attenuate the effects of transient spatial attention on temporal resolution. *Vision Research, 44*(12), 1375-1387.

Zele, A. J., Pokorny, J., Lee, D. Y., & Ireland, D. (2007). Anisometropic amblyopia: Spatial contrast sensitivity deficits in inferred magnocellular and parvocellular vision. *Investigative Ophthalmology & Visual Science, 48,* 3622–3631.

APPENDIX A

PILOT EXPERIMENT

In this experiment, the feasibility of using the DTI measure was evaluated. The DTI data was expected to provide a better understanding of the stimulus factors that affected when a targets reappear in the artificial scotoma paradigm. In this experiment, a traditional scotoma inducing display with two target sizes and three temporal frequencies was tested to a) replicate the TTF duration and b) see if DTI will produce measureable differences for the two manipulations. Target size and background flicker rate have consistently shown significant difference in previous studies (De Weerd et al., 1998). The large target size of 4° visual angle with the stationary random dot background was expected to fade slowly as compared to the smaller target size of 2° with the background flickering at higher temporal speed (Ramachandran et al., 1993; De Weerd et al., 1998). All targets at 10° eccentricity in the periphery. The target was randomly placed at either top right or bottom right corner of the display to minimize any confounding effect of adaptation to a fixed retinal location.

Methods

Participants

Three adults (one female, 21 to 25 years old) with normal or corrected-to-normal vision gave written informed consent to participate in the study. They and were classified as right-handed according to the Annett Handedness Scale or were right eye dominant.

Stimuli and Apparatus

Images and videos were presented on a 21-inch LCD monitor (60 Hz) using Quick Time player. Participants were seated in a dimly lit room 50 cm from the monitor viewing images or videos that subtended a visual angle of 42° x 32° using a chin and forehead-rest.

The right eye blind spot of each participant was mapped in the same manner as described in Experiment 1. The experimental stimulus consisted of a homogenous grey square target, blue dot at the blind spot, and a red fixation cross on a random dot background flickering at different temporal speeds. A MATLAB program was used to create images containing randomly placed 50% black and 50% white dots. The video clips had an average luminance of 45 cd/m^2. The targets were equiluminant to the grey square target subtending either 2° or 4° of visual angle. The targets were placed 10° away from the fixation, either in the top right or bottom right quadrant.

Procedure

The participants were instructed to fixate while viewing the display monocularly (right eye). The investigator initiated each trial by pressing the spacebar on a computer keyboard. Two stopwatch timers recorded the TTF and DTI response during each trial. The investigator operated one stopwatch while the participant operated other. The investigator started the first timer at the beginning of each trial and recorded the time until target filling-in. The participants started their timer when the target became invisible and stopped the timer as soon as the target was visible again. The trial ended as soon as the participants stopped their timer. The first timer measured TTF and the second timer measured the DTI in each trial. The data was collected in two session with a total of 24 practice and 120 experimental trial.

Results

The trials where the blind spot stimulus was visible to the participant were excluded from the analysis. The data showed that both the factors affected the time-to-fade and the duration of invisibility. As expected, the target size of 4° (M = 10.62, SEM = 1.15) consistently took longer to fade as compared to 2° (M = 6.47, SEM = 0.80) for all temporal speeds (t (2) = 6.58, $p < 0.05$). In addition, the time taken to fade was longest for stationary displays (M = 10.21, SEM = 1.91) and shortest for the 20 fps high temporal speed condition (M = 7.19, SEM = 0.39) (t (2) = 2.16, p = 0.08). These differences in the time taken by a target to fade due to changes in target size and background flicker rate were consistent with the results from previous studies. The duration of target invisibility showed a trend in the response times that was dependent on the target size and background flicker rate. In the stationary displays condition, targets remained invisible (t (2) = 3.32, $p < 0.05$) for a longer period (M = 14.01, SEM = 1.46) as compared to the 20 fps condition (M = 10.83, SEM = 1.79). In addition, the smaller targets remained invisible for a longer duration (M = 13.49, SEM = 2.27) as compared to bigger targets (M = 10.64, SEM = 1.83) (t (2) = 2.43, p = 0.07). Thus, larger targets on both static and flickering backgrounds caused TTF to increase as compared to small targets. On the other hand, large targets on both static and flickering background reappeared faster than small targets. The data suggests that the duration of target invisibility might be a useful and informative measure for the Experiments 1, 2 and 3.

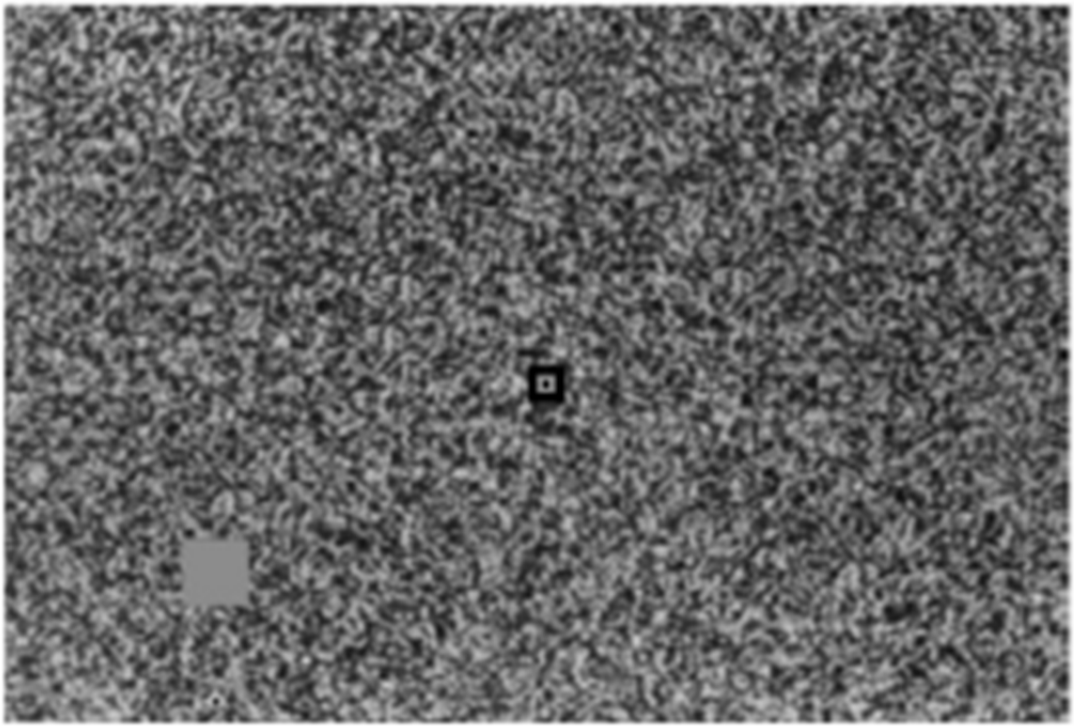

Figure 1. *Example of an artificial scotoma display*. The display contains a black fixation and a grey square target in the periphery on a twinkling random dot background (Ramachandaran & Gregory, 1991).

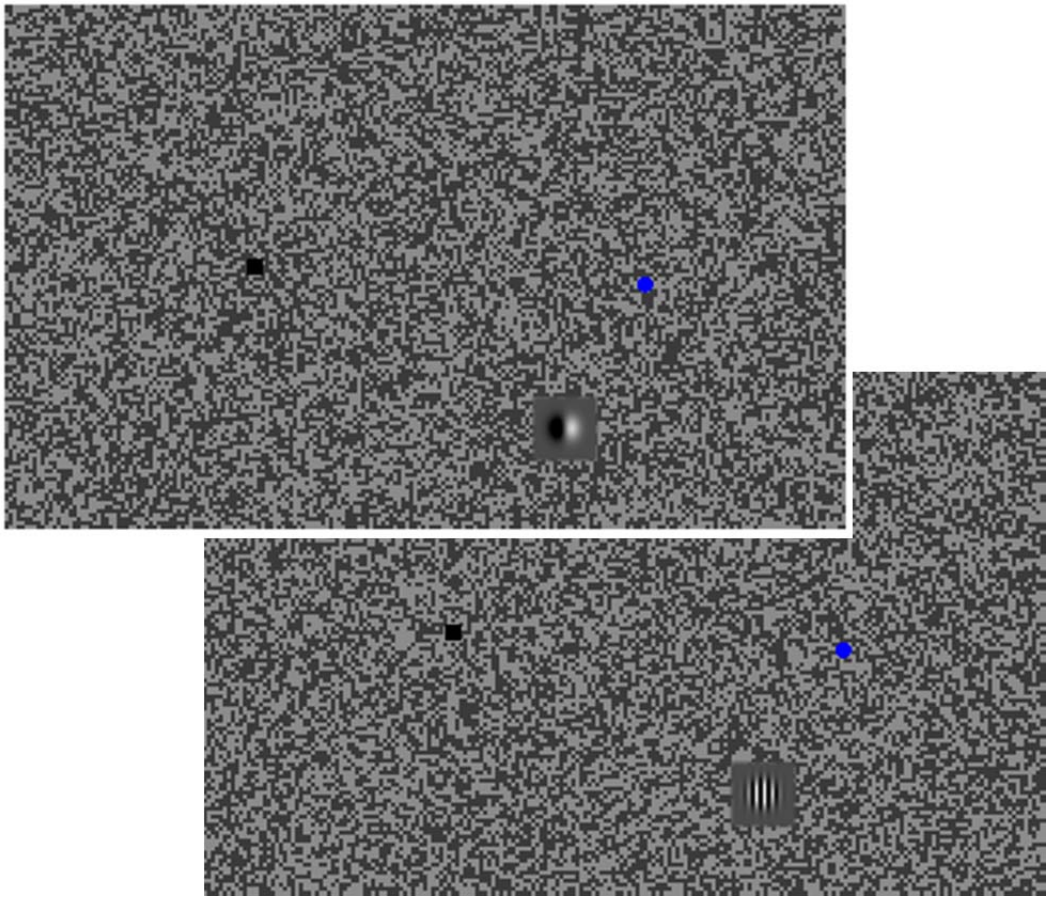

Figure 2. Example of random dot display (Experiment 1). Customized display with either 0.5 cpd target region (top) or 4 cpd target region (bottom).

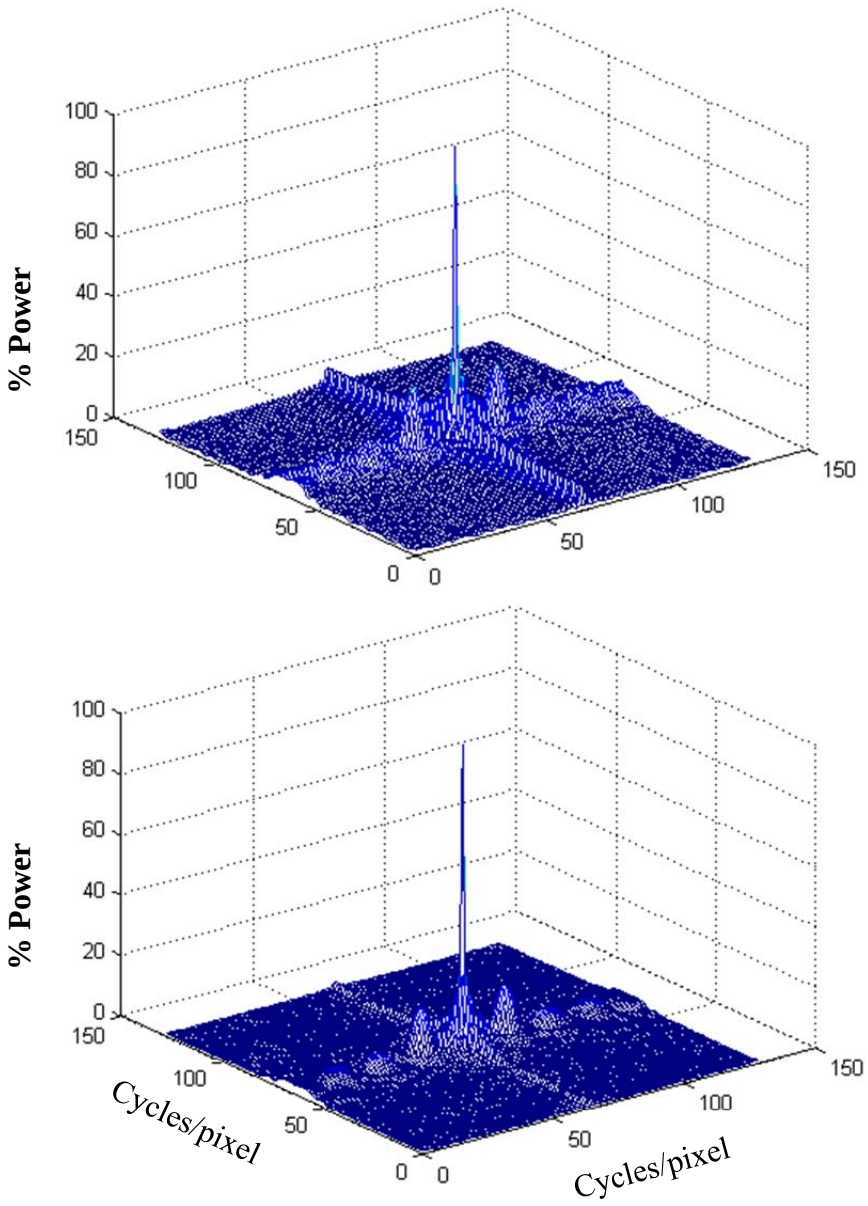

Figure 3. Power spectrum plots for 4 cpd target. Top graph shows % power spectrum for sharp edge target region and bottom plot show % power for blurred edge target.

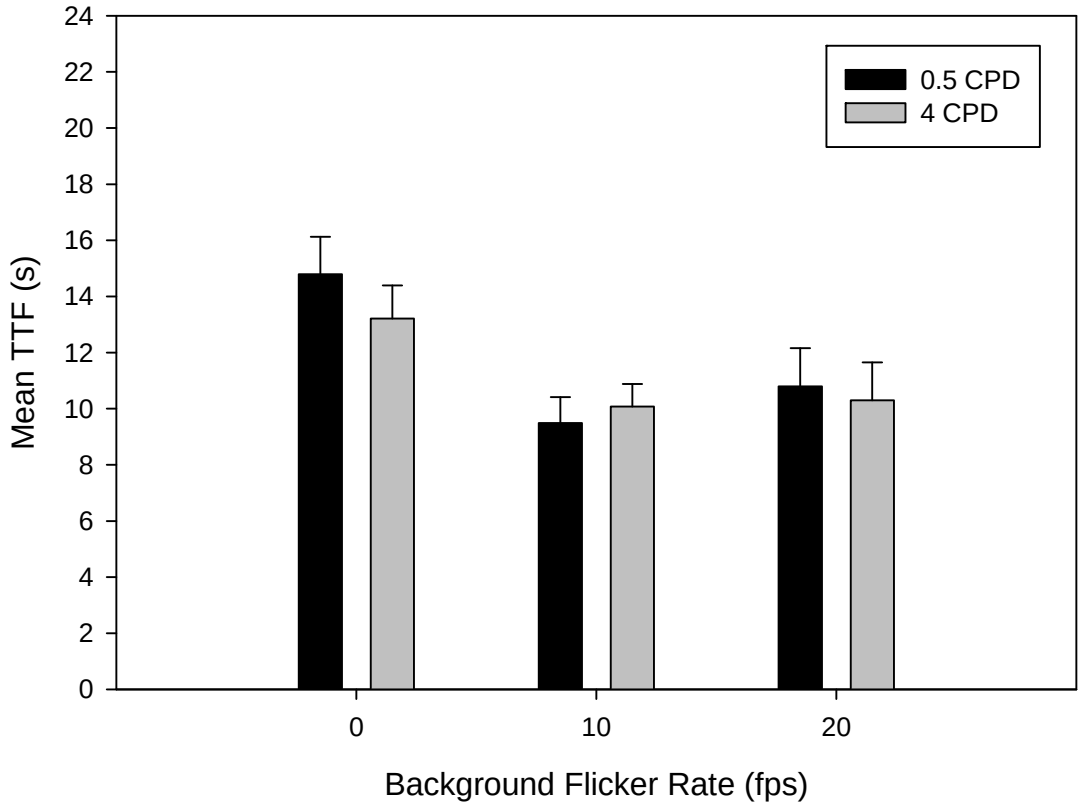

Figure 4. TTF data for Experiment 1. The effect of different background speeds and spatial frequency of target on time taken to fade (n = 11).

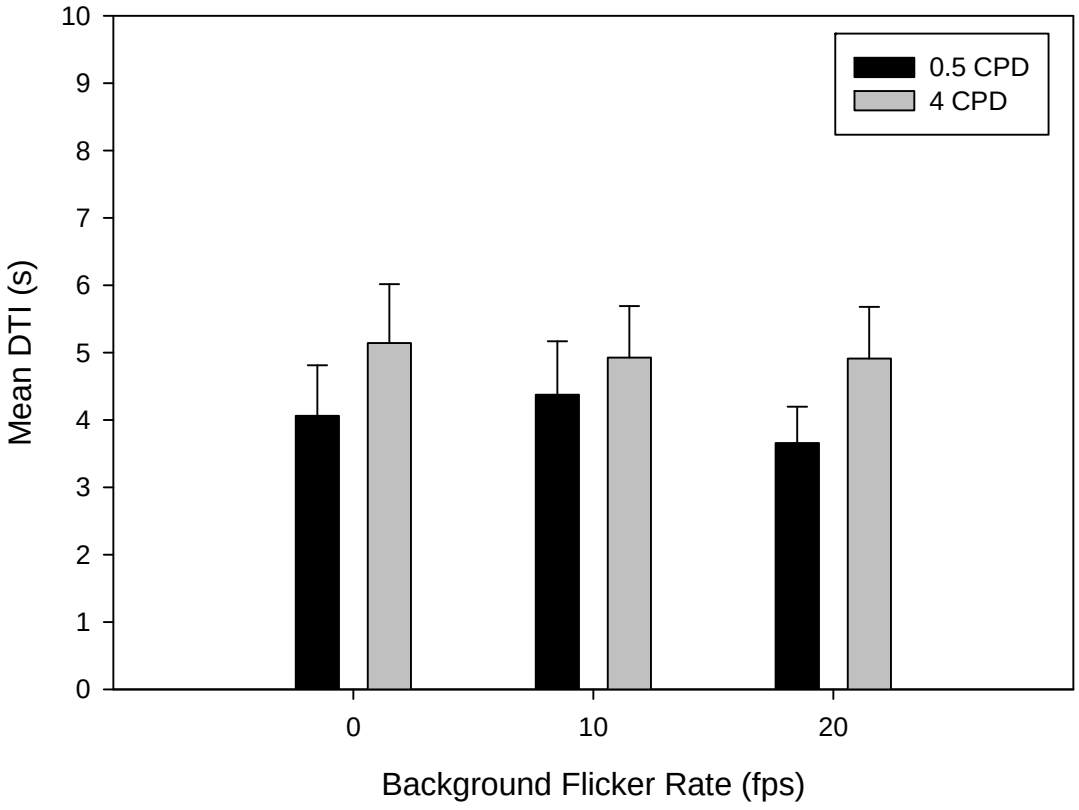

Figure 5. DTI data for Experiment 1. The effect of different background speeds and spatial frequency of target on time taken for targets to reappear (n = 11).

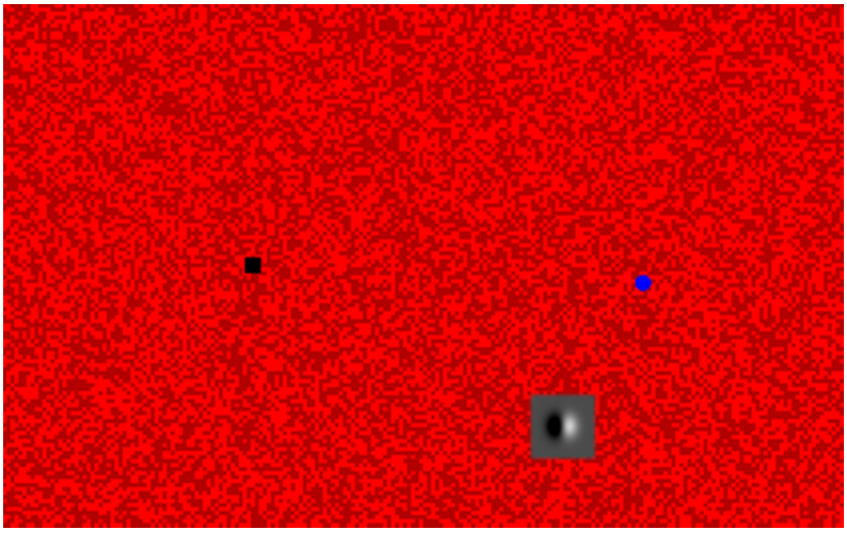

Figure 6. Example of red random dot display (Experiment 2). Customized artificial scotoma display used in chromatic condition.

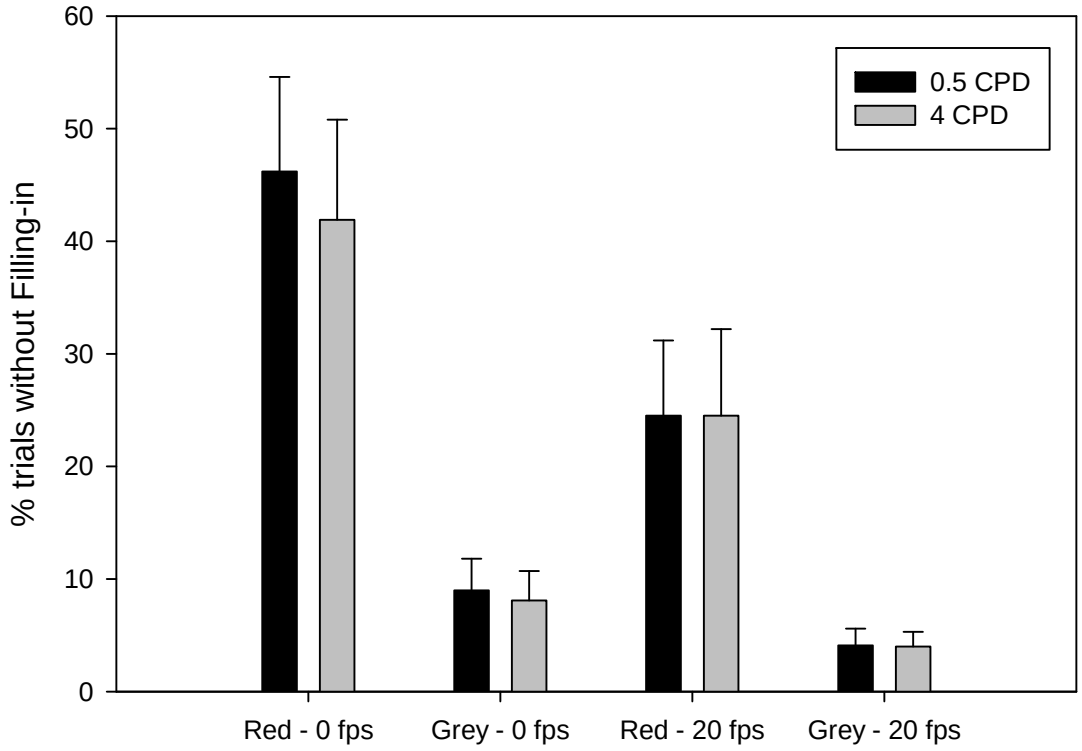

Figure 7. Percent trials without filling-in for Experiment 2. Percentages are plotted as a function of background flicker rate and color (n=11).

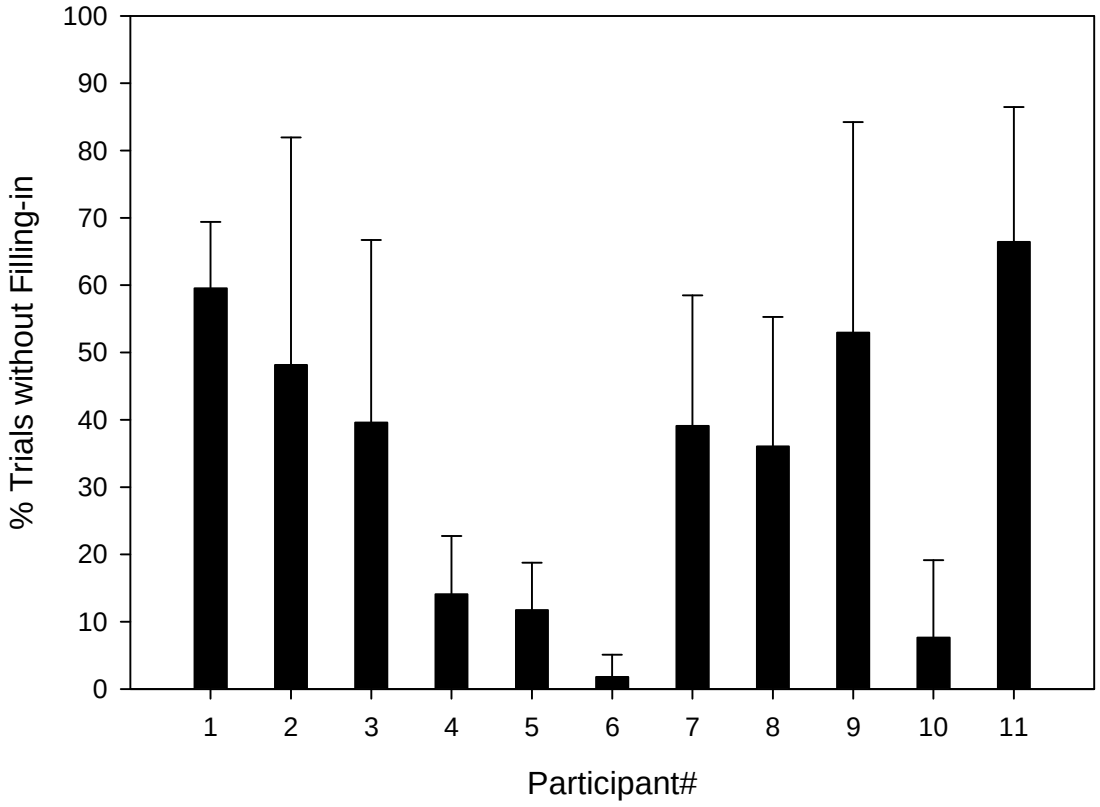

Figure 8. Percent trials without filling-in for Experiment 2. Percent trials without filling-in across all conditions plotted for each participant with error bars indicating standard deviations (n=11).

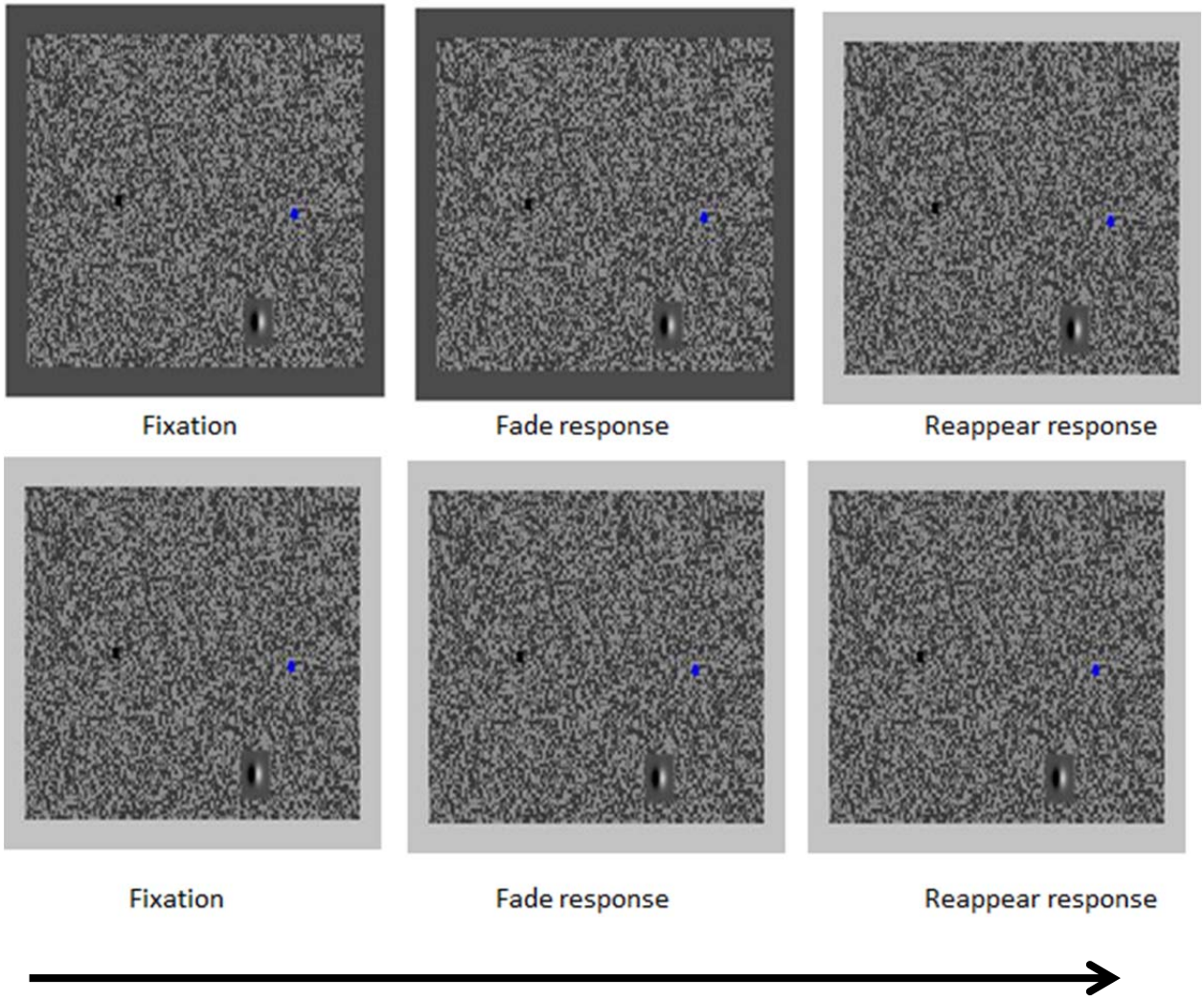

Figure 9. Experiment 3 trial sequence. Examples of a modified steady (bottom row) and pulsed pedestal (top row) trials using a surround pedestal.

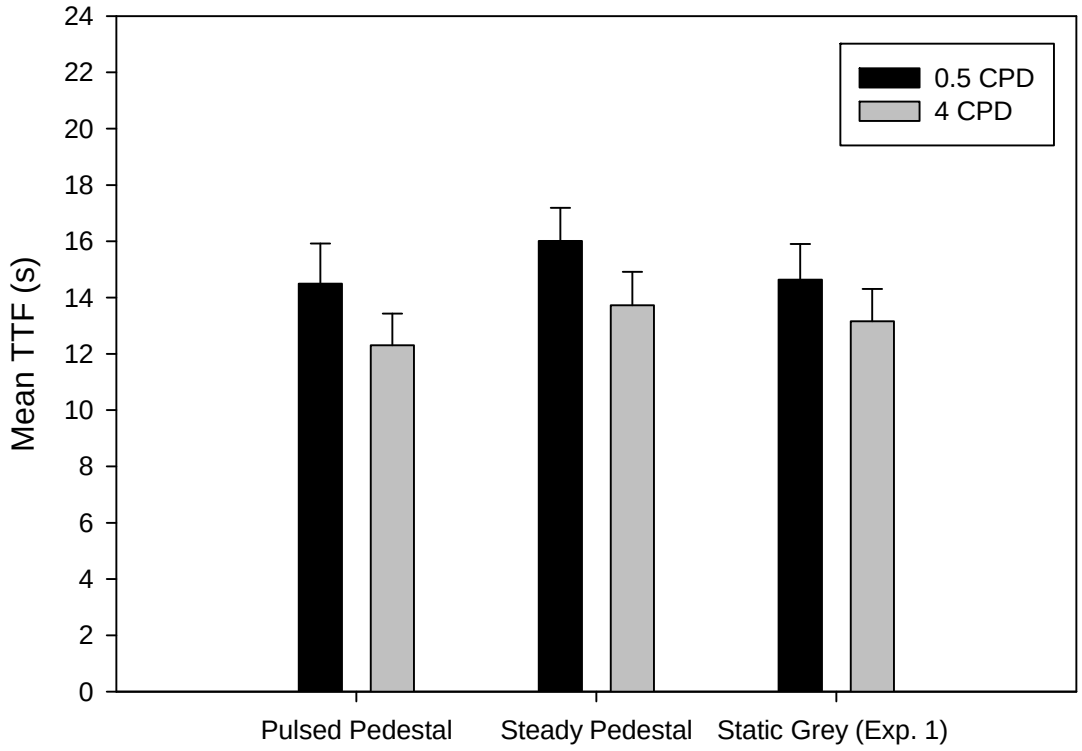

Figure 10. TTF data for Experiment 3. TTF plotted as a function of SF of target region in steady and pulsed backgrounds compared to full grey background from Experiment 1 (n= 12).

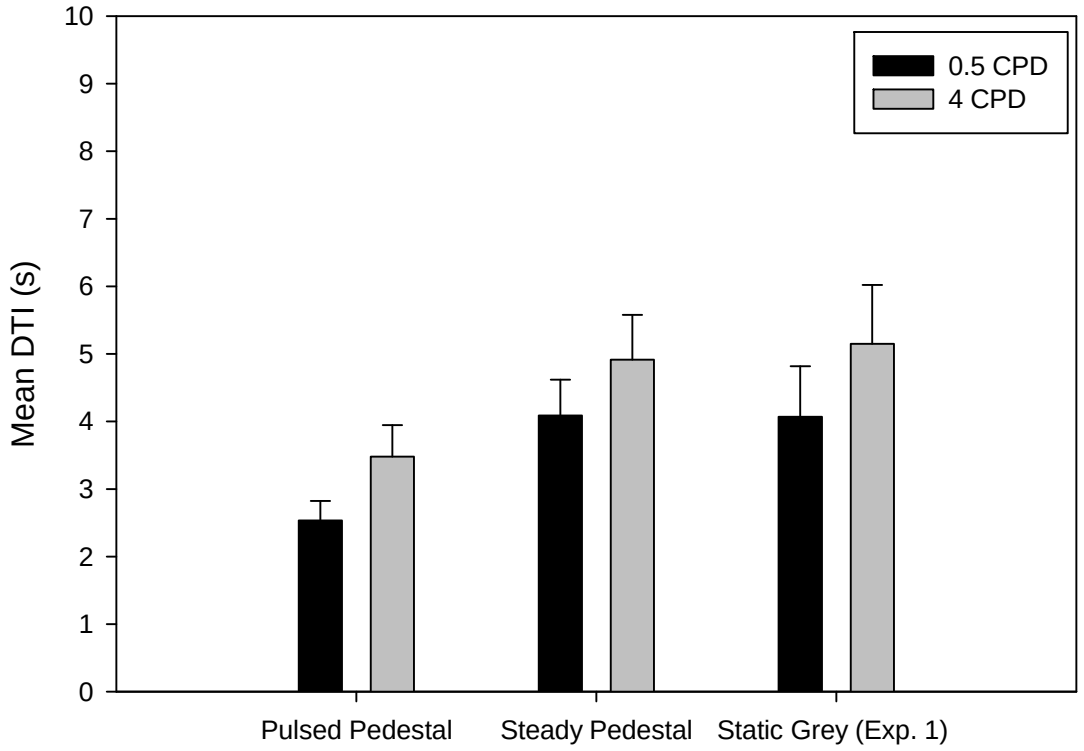

Figure 11. DTI data for Experiment 3. TTF plotted as a function of SF of target region in steady and pulsed backgrounds compared to full grey background from Experiment 1 (n= 12).